

1 **Functional role of Polymerase IV during pollen development in *Capsella***

2 Zhenxing Wang^{1*}, Nicolas Butel^{1*}, Juan Santos-González¹, Filipe Borges^{2,3}, Jun Yi¹,
3 Robert A. Martienssen², German Martinez¹, Claudia Köhler¹

4 ¹ Department of Plant Biology, Swedish University of Agricultural Sciences and Linnean
5 Center for Plant Biology, Uppsala 75007, Sweden

6 ² Howard Hughes Medical Institute and Cold Spring Harbor Laboratory, 1 Bungtown
7 Road, Cold Spring Harbor, New York 11724, USA.

8 ³ Present address: Institut Jean-Pierre Bourgin, INRA, AgroParisTech, Université Paris-
9 Saclay, 78000, Versailles, France

10 *both authors contributed equally to this work

11 Corresponding Author: Claudia.Kohler@slu.se

12

13 **Short title:** Requirement of Polymerase IV in *Capsella* pollen.

14 **One-sentence summary:** Loss of Polymerase IV function in *Capsella rubella* causes
15 microspore arrest, revealing an important functional role of Polymerase IV during pollen
16 development.

17 The author responsible for distribution of materials integral to the findings presented in
18 this article in accordance with the policy described in the Instructions for Authors
19 (www.plantcell.org) is: Claudia Köhler (Claudia.Kohler@slu.se)

20

21

22

23

24 **Abstract**

25 In *Arabidopsis thaliana*, the DNA-dependent RNA polymerase IV (Pol IV) is required for
26 the formation of transposable element (TE)-derived small RNA (sRNA) transcripts. These
27 transcripts are processed by DICER-LIKE 3 into 24-nt small interfering RNAs (siRNAs)
28 that guide RNA-dependent DNA methylation. In the pollen grain, Pol IV is also required
29 for the accumulation of 21/22-nt epigenetically-activated siRNAs (easiRNAs) that likely
30 silence TEs by post-transcriptional mechanisms. Despite this proposed functional role,
31 loss of Pol IV function in *Arabidopsis* does not cause a discernable pollen defect. Here,
32 we show that loss of *NRPD1*, encoding the largest subunit of Pol IV in the Brassicaceae
33 *Capsella rubella*, causes post-meiotic arrest of pollen development at the microspore
34 stage. As in *Arabidopsis*, all TE-derived siRNAs were depleted in *Capsella nrpd1*
35 microspores. In wild-type background, we found that the same TEs produced 21/22-nt
36 and 24-nt siRNAs, leading us to propose that Pol IV is generating the direct precursors
37 for 21-24-nt siRNAs, which are targeted by different DICERs. Arrest of *Capsella nrpd1*
38 microspores was accompanied by deregulation of genes targeted by Pol IV-dependent
39 siRNAs. The distance of TEs to genes was much closer in *Capsella rubella* compared to
40 *Arabidopsis thaliana*, providing a possible explanation for the essential role of Pol IV for
41 pollen development in *Capsella*. Our study in *Capsella* uncovers a functional requirement
42 of Pol IV in microspores, emphasizing the relevance of investigating different plant
43 models.

44

45

46

47

48

49

50

51 **Introduction**

52 In flowering plants, male and female gametes are the products of a multistep process that
53 starts from a cell undergoing a meiotic division resulting in haploid spores dividing
54 mitotically to form multicellular gamete-containing gametophytes. The pollen grain
55 corresponds to the male gametophyte and forms after two mitotic divisions of the haploid
56 microspore. The first mitotic division generates the large vegetative cell and a small
57 generative cell that after another mitotic division will give rise to the two sperm cells. The
58 second mitotic division can occur before pollen germination, like in *Arabidopsis thaliana*,
59 or during pollen germination (Berger and Twell, 2011). Unlike in the male lineage where
60 all microspores will develop into pollen, in most flowering plants only one megasporangium
61 survives and mitotically divides to give rise to the seven-celled female gametophyte
62 containing the two female gametes, the egg cell and the central cell (Tekleyohans et al.,
63 2017). In contrast to animals where germ cells separate early from the somatic lineage,
64 plant germ cells originate from differentiated cells that acquire the competence to undergo
65 meiotic divisions (Schmidt et al., 2015) The formation of male and female plant gametes
66 is connected with a partial resetting of epigenetic marks that likely serves to achieve
67 meiotic competence (Borges and Martienssen, 2013; Baroux and Autran, 2015; Borg and
68 Berger, 2015). Epigenetic modifications can be applied directly on the DNA in the form of
69 DNA methylation, or on histones, the proteins that package DNA into nucleosomes. The
70 specific type of the modification and its position on the genomic locus defines the
71 transcriptional outcome. DNA methylation is generally (but not always) a repressive
72 modification and is used to silence transposable elements (TEs), but also genes during
73 specific stages of plant development. In plants, DNA methylation can occur in CG, CHG,
74 and CHH context (where H correspond to A, T or C) and is established and maintained
75 by different DNA methyltransferases. Methylation in CG context is maintained by the
76 METHYLTRANSFERASE 1 (MET1), while CHG methylation maintenance requires
77 CHROMOMETHYLASE 3 (CMT3) and to a lesser extent CMT2 (Zhang et al., 2018). The
78 RNA-dependent DNA methylation (RdDM) pathway maintains CHH methylation by
79 recruiting the DOMAINS REARRANGED METHYLTRANSFERASE 2 (DRM2). This
80 pathway requires the plant-specific DNA-dependent RNA polymerases (Pol) IV and V
81 (Herr et al., 2005; Onodera et al., 2005; Xie et al., 2004). Pol IV generates small

82 transcripts of about 30-40-nt in size that are converted into double stranded RNA by the
83 action of the RNA-DEPENDENT RNA POLYMERASE 2 (RDR2) (Blevins et al., 2015;
84 Zhai et al., 2015a; Li et al., 2015). These double stranded RNAs are processed into 23-
85 and 24-nt siRNAs by DICER-LIKE 3 (DCL3) (Xie et al., 2004; Singh et al., 2019). The 24-
86 nt siRNAs preferentially associate with ARGONAUTE4 (AGO4) and guide DRM2 to its
87 targets by associating with Pol V transcripts (Cao and Jacobsen, 2002; Zilberman et al.,
88 2003; Wierzbicki et al., 2009). Recent studies further uncovered that Pol IV is required for
89 the accumulation of 21/22-nt epigenetically activated siRNAs (easiRNAs) in pollen and
90 establishes a hybridization barrier between plants of different ploidy grades (Martinez et
91 al., 2018; Borges et al., 2018; Satyaki and Gehring, 2019).

92 Pollen formation in *Arabidopsis* is connected with reprogramming of CHH methylation.
93 There is a strong reduction of CHH methylation during meiosis, which is followed by a
94 restoration of CHH methylation in the pollen vegetative cell and a locus-specific
95 restoration in sperm (Calarco et al., 2012; Ibarra et al., 2012; Walker et al., 2018).
96 Nevertheless, CHH methylation is not completely erased during meiosis and locus-
97 specific CHH methylation was shown to be of functional relevance for meiosis (Walker et
98 al., 2018). In *Arabidopsis*, the accumulation of meiosis-specific sRNAs depends on Pol
99 IV (Huang et al., 2019) and meiotic defects have been reported in RdDM mutants *rdr2*,
100 *drm2*, and *ago4*, albeit at low frequency in the Columbia (Col) accession (Oliver et al.,
101 2016; Walker et al., 2018). There is furthermore a relaxation of heterochromatin occurring
102 in the vegetative cell as a consequence of histone H1 depletion, which allows the DNA
103 demethylase DEMETER (DME) to access and demethylate TEs in the vegetative cell
104 (Slotkin et al., 2009; He et al., 2019). Demethylated TEs in the vegetative cell generate
105 siRNAs that can move to sperm cells and may serve to enforce TE silencing in sperm
106 (Martinez et al., 2016; Ibarra et al., 2012; Kim et al., 2019). Nevertheless, the functional
107 relevance of enhanced TE silencing in sperm by mobile siRNAs remains to be
108 demonstrated, since loss of DME function in pollen causes a pollen germination defect,
109 but not a seed defect (Schoft et al., 2011).

110 *Arabidopsis thaliana* differs from many other species by its low repeat content of about
111 24% of the 135-Mb genome (Maumus and Quesneville, 2014), which may explain its

112 apparent tolerance to the lack of Pol IV and other RdDM components. Like *Arabidopsis*
113 *thaliana*, the closely related Brassicaceae *Capsella rubella* is a selfer; however, because
114 of its recent transition to selfing (30-100 k years ago (kya)) it has maintained high numbers
115 of TEs and almost half of the 219-Mb genome is repetitive, with many TEs being located
116 in the vicinity to genes (Slotte et al., 2013; Foxe et al., 2009; Guo et al., 2009; Niu et al.,
117 2019). In contrast, *Arabidopsis thaliana* became a selfer around 500 kya and experienced
118 a strong reduction of TEs (de la Chaux et al., 2012). Given the different TE content in
119 both species, we hypothesized that loss of Pol IV function may have a stronger impact in
120 *Capsella rubella*. To test this hypothesis, we generated a loss-of-function allele in the
121 *Capsella rubella* Pol IV subunit NRPD1. We found that loss of NRPD1 in *Capsella* caused
122 impaired male fertility, as a consequence of a post-meiotic arrest of pollen at the
123 microspore stage. Wild-type microspores accumulated Pol IV-dependent siRNAs in the
124 size range of 21-24-nt, suggesting that the formation of easiRNAs is initiated during or
125 after meiosis. In *Capsella* and *Arabidopsis* microspores, 21/22-nt and 24-nt siRNAs were
126 generated from the same TE loci, suggesting that Pol IV is producing the precursors for
127 both types of siRNAs. Consistently, we found that loss of DCL3 in *Arabidopsis* causes
128 increased formation of 21/22-nt siRNAs, supporting the idea that different DCLs compete
129 for the same double stranded RNA precursor molecule. Microspore arrest in *Capsella*
130 *nRPD1* mutant plants correlated with a substantially stronger deregulation of genes
131 compared to *Arabidopsis nRPD1* microspores, including known regulators of pollen
132 development. We conclude that Pol IV in *Capsella* generates siRNAs in the size range of
133 21-24-nt that have important functional roles for pollen development.

134 **Results**

135 **Loss of Pol IV function causes microspore arrest in *Capsella***

136 To test the functional role of Pol IV in *Capsella rubella*, we generated a knockout mutant
137 in the NRPD1 subunit of Pol IV using Crispr/Cas9 (now referred to as *Cr nRPD1*) (Figure
138 1A). The induced deletion caused the formation of a frameshift and a stop codon after
139 385 amino acids, leading to a truncated protein without the catalytically active site
140 (Onodera et al., 2005) that is likely a functional null allele. Like in the *Arabidopsis thaliana*
141 *nRPD1* mutant (referred to as *At nRPD1*), TE-derived 24-nt siRNAs were abolished in *Cr*

142 *nrpd1* leaves (Figure 1B) (Wierzbicki et al., 2012), connected with a strong reduction of
143 CHH methylation levels over TEs (Figure 1C). These results reveal that Pol IV has a
144 conserved function in siRNAs biogenesis and is required for RdDM in *Capsella* and
145 *Arabidopsis*.

146 Strikingly, homozygous *Cr nrpd1* had strongly reduced seed set (Figure 2A), on average
147 *Cr nrpd1* siliques contained only three seeds, corresponding to about 25% of normal wild-
148 type seed set. We found that male fertility of *Cr nrpd1* was strongly impaired, with most
149 pollen being arrested after meiosis at the microspore stage (Figure 3A-K). Only
150 homozygous *Cr nrpd1* mutants were impaired in pollen development, while heterozygous
151 *Cr nrpd1* plants were completely fertile and pollen development was normal (Figure 3C,
152 G, K), indicating that loss of Pol IV function affects a stage prior to microspore
153 development, or alternatively, affects tapetum development. Cross-sections of
154 microsporangia confirmed that *Cr nrpd1* mainly formed arrested microspores, with
155 approximate 20% of the pollen were able to complete development (Figure 3L). There
156 were no obvious differences in tapetum development and degradation in *Cr nrpd1*
157 compared to wild type (Figure 3M-T).

158 Consistent with previous work showing a maternal effect of *nrpd1* mutants in *Brassica*
159 *rapa* (Grover et al., 2018), about 30% of ovules of homozygous *Cr nrpd1* remained
160 unfertilized after pollination with wild-type pollen, while there was no statistically
161 significant fertility decrease in heterozygous *Cr nrpd1* (Figure 2B-E). Inspection of ovules
162 of *Cr nrpd1* did not reveal obvious abnormalities; wild-type and *Cr nrpd1* ovules contained
163 both an egg cell and unfused polar nuclei at 2 days after emasculation (Figure 2F-H).
164 Furthermore, *Cr nrpd1* homozygous, but not heterozygous plants had strongly reduced
165 seed size after self-fertilization or pollination with wild-type pollen (Figure 2I-L), revealing
166 a maternal effect on ovule and seed development.

167 Complementation of *Cr nrpd1* with the *Arabidopsis NRPD1* genomic sequence under
168 control of the constitutive *RPS5A* promoter (Weijers et al., 2001) fully restored pollen
169 development in the T1 generation of transgenic plants (Figure 3D,H,L), confirming that
170 the pollen defect is a consequence of impaired Pol IV function and that NRPD1 is
171 functionally conserved in *Arabidopsis* and *Capsella*.

172 Meiotic abnormalities at low frequency were previously reported for mutants of the RdDM
173 pathway in *Arabidopsis* (Oliver et al., 2016; Walker et al., 2018). However, we did not
174 detect abnormal chromosome segregation during male meiosis in *Cr nrpd1*
175 (Supplemental Figure 1) and inspection of meiotic products revealed the formation of
176 tetrads (Supplemental Figure 2), indicating that the pollen arrest after meiosis is not a
177 consequence of a chromosome segregation defect.

178

179 **Pol IV-dependent silencing of TEs in *Capsella* microspores**

180 The arrest of *Cr nrpd1* pollen at the microspore stage prompted us to compare sRNAs of
181 wild-type and *Cr nrpd1* microspores. We enriched for microspores using a percoll gradient
182 following previously established procedures (Dupl'akova et al., 2016). On average, the
183 purity of the fractions was 84% (Supplemental Figure 3A). Sequencing of isolated sRNAs
184 revealed that TE-derived siRNAs in the size range of 21-24-nt were abolished in *Cr nrpd1*
185 microspores (Figure 4A, Supplemental Figure 4A). Like previously described for
186 *Arabidopsis* meiocytes (Huang et al., 2019), we observed a strong accumulation of 23-nt
187 siRNAs in *Capsella* microspores (Figure 4A, Figure 5A). Nearly all TE loci generating
188 21/22-nt siRNAs also formed 24-nt siRNAs (Figure 4B). To test the functional role of Pol
189 IV-dependent siRNAs in TE silencing, we isolated RNA from wild-type and mutant
190 microspores and performed an RNA-seq analysis. Those TEs that lost 21/22- and 24-nt
191 siRNAs, had higher transcript levels in *Cr nrpd1* microspores compared to wild type
192 (Figure 4C), revealing a role of Pol IV-dependent siRNAs in TE silencing in microspores.
193 Together, we conclude that Pol IV-dependent TE-derived siRNAs in the size range of 21-
194 24-nt are present in microspores and are required for TE silencing. This is consistent with
195 recent work proposing that pollen easiRNAs are produced during or shortly after meiosis
196 (Borges et al., 2018).

197 **Pol IV-dependent siRNAs also accumulate in *Arabidopsis* microspores**

198 Previous work demonstrated that Pol IV generates small transcripts in the size range of
199 30-40-nt that are converted into 24-nt siRNAs by the action of DCL3 (Zhai et al., 2015a;
200 Blevins et al., 2015; Yang et al., 2016). To be able to genetically dissect the Pol IV-

201 dependent pathway leading to the formation of siRNAs in the size range of 21-24-nt, we
202 tested for the presence of similar siRNAs in *Arabidopsis* microspores.

203 We sequenced sRNAs from *Arabidopsis* wild-type and *nrpd1* microspores that had been
204 enriched to 90% following the same procedures as applied for *Capsella* (Supplemental
205 Figure 3B, Supplemental Figure 4B). Like in *Capsella* microspores, *Arabidopsis*
206 microspores accumulated TE-derived siRNAs in the size range of 21-24-nt that were
207 abolished in *At nrpd1* microspores (Figure 4D). Thus, 21/22-nt TE-derived siRNAs are
208 already present in microspores and depend on Pol IV, strongly supporting the idea that
209 biogenesis of easiRNAs present in mature pollen starts at an earlier stage, most likely
210 during meiosis. Consistently, microspores and meiocytes as well as microspores and
211 mature pollen grains share a large number of loci generating Pol IV-dependent siRNAs
212 (Figure 5C, D).

213 To test the functional requirement of Pol IV-derived siRNAs in TE silencing, we correlated
214 the TEs producing Pol IV-dependent 21/22-nt and 24-nt siRNAs to TE expression
215 changes in *At nrpd1*, lacking Pol IV function. We found a significant association between
216 Pol IV-dependent siRNAs and expression change of TEs in *At nrpd1* microspores (Figure
217 6A) similar to *Capsella* (Figure 4C), revealing that TE-derived siRNAs are involved in the
218 repression of TE expression in microspores.

219 Pol IV is usually associated with 24-nt siRNAs through the RdDM pathway and its strong
220 effect on the production of 21/22-nt siRNAs in pollen is thus unexpected. One hypothesis
221 could be that Pol IV transcripts are direct precursors of 21/22-nt siRNAs. If true, we
222 expected that microspore TE-derived 21/22-nt and 24-nt siRNAs should arise from the
223 same genomic loci. Consistently, like in *Capsella* microspores (Figure 4B), nearly all TE
224 loci generating 21/22-nt siRNAs also formed 24-nt siRNAs (Figure 6B). Visualizing the
225 individual reads in a genome browser showed that all read sizes accumulated along the
226 same loci (Supplemental Figure 5). Taken together, this data show that TE-derived 21/22-
227 nt siRNAs and 24-nt siRNAs are produced from the same loci in a Pol IV-dependent
228 manner and are able to repress TEs in both *Capsella* and *Arabidopsis*.

229

230 **TE-derived siRNAs in microspores require RDR2 activity**

231 TE-derived siRNAs were produced from both DNA strands (Figure 6C and Supplemental
232 Figure 5), suggesting the involvement of an RNA-dependent RNA polymerase in the
233 production of the double stranded RNAs used as template for the microspore TE-derived
234 siRNA production.

235 Among the three RDRs with known function in *Arabidopsis*, RDR2 is tightly associated
236 with Pol IV (Li et al., 2015; Zhai et al., 2015a) and RDR6 has been shown to affect some
237 easiRNAs (Creasey et al., 2014; Martinez et al., 2018). To assess the potential
238 involvement of RDR2 and RDR6 in TE-derived siRNA production in microspores, we
239 analyzed publically available sRNA sequencing data from *rdr2* and *rdr6* inflorescences
240 (Zhai et al., 2015a; Panda et al., 2016). The sRNA pattern of wild-type and *At nrpd1*
241 inflorescence tissues was comparable to that of microspores (Figure 4D and Figure 6D),
242 indicating that the siRNAs identified in *rdr2* and *rdr6* inflorescences are comparable to
243 those of microspores. While *rdr6* had no effect on the distribution of TE-derived siRNAs,
244 in *rdr2* inflorescences the accumulation of TE-derived siRNAs was abolished (Figure 6D),
245 indicating that RDR2 is likely involved in TE siRNA biogenesis. We also generated siRNA
246 profiles from *rdr2* and *rdr6* pollen (Figure 5B), which confirm the data obtained from
247 inflorescences and reveal that RDR2, but not RDR6 is required for the generation of
248 21/22-nt siRNAs. These results reinforce the idea that 21/22-nt and 24-nt TE-derived
249 siRNAs present in pollen are processed from a double stranded RNA produced by Pol IV
250 and RDR2.

251 **DICERs producing TE-derived siRNAs compete for the same double stranded
252 RNA template**

253 Our data suggests that TE-derived siRNAs of different size classes are derived from
254 double stranded RNAs produced by Pol IV/RDR2 (Figure 6B). We hypothesized that the
255 production of different size classes of siRNAs is a consequence of different DICERs
256 competing for the same double stranded RNA template, as it has been previously shown
257 to occur upon disruption of DCL3 function (Gascioli et al., 2005; Henderson et al., 2006;
258 Kasschau et al., 2007; Bond and Baulcombe, 2015). If true, the impairment of DCL3

259 should increase the proportion of Pol IV-dependent 21/22nt siRNAs accumulating over
260 defined loci.

261 To test this idea, we used publically available sRNA sequencing data of *dcl3*
262 inflorescences (Li et al., 2015). We quantified the number of normalized 21/22-nt siRNAs
263 and 24-nt siRNAs mapped against TEs in wild-type and *dcl3* inflorescences. In wild type,
264 24-nt siRNAs were the most abundant siRNA, exceeding the level of 21/22-nt siRNAs by
265 nearly seven fold (Figure 6E). In *dcl3*, the abundance of 21/22-nt siRNAs was highly
266 increased, while 24-nt siRNAs were depleted (Figure 6E). To rule out that the increased
267 abundance of 21/22-nt siRNAs is a consequence of a normalization artifact, we performed
268 the same analysis with miRNAs. As DCL3 is not involved in the 21/22-nt miRNA pathway,
269 observed changes would be suggestive for a normalization artifact. The abundance of
270 21/22-nt miRNAs was highly similar in wild type and *dcl3* (Figure 6F), strongly supporting
271 the notion that the observed increase of 21/22-nt siRNAs in *dcl3* inflorescences is not a
272 consequence of a normalization problem. These results indicate that there is indeed a
273 competition between DCL3 and other DCLs for the same double stranded RNA precursor,
274 in agreement with previous data (Gascioli et al., 2005; Henderson et al., 2006; Kasschau
275 et al., 2007; Bond and Baulcombe, 2015).

276 **TE-derived siRNAs are highly enriched at *COPIA95* in *Capsella* microspores**

277 To investigate whether Pol IV-dependent siRNAs target similar loci in *Arabidopsis* and
278 *Capsella*, we identified sRNA reads mapping to both genomes, which were then mapped
279 to 527 *Arabidopsis* TE consensus sequences previously reported (Repbase) (Bao et al.,
280 2015). We found a similar number of TE families accumulating Pol IV-dependent siRNAs
281 in *Arabidopsis* and *Capsella* microspores, (316 and 301 TE families, respectively), of
282 which 225 were common between both species (Figure 7A). There were substantially
283 fewer TE families forming 24-nt siRNAs in *Capsella* microspores (133) compared to
284 *Arabidopsis* (303), but the majority of those overlapped between both species (103).
285 Nearly all TE families forming 24-nt siRNAs also formed 21/22-nt siRNAs (94.1% (285
286 out of 303 TE families) in *Arabidopsis* and 99.2% (132 out of 133 TE families) in *Capsella*)
287 (Figure 7A), supporting the idea that 21/22-nt siRNAs and 24-nt siRNAs are derived from
288 the same TE loci in microspores.

289 To investigate the specificity of TE-derived siRNAs in *Arabidopsis* and *Capsella*
290 microspores, we calculated the proportion of siRNAs targeting specific TE families.
291 Strikingly, we found that nearly 20% of 21/22-nt siRNAs and more than 40% of 24-nt
292 siRNAs were derived from the *COPIA95* family (*COPIA95* long-terminal repeats (LTR)
293 and internal (I)) in *Capsella* microspores, while only 0.3% of both siRNA classes were
294 derived from *COPIA95* in *Arabidopsis* microspores (Figure 7B). We identified 17 and 70
295 TEs accumulating *COPIA95*-derived Pol IV-dependent siRNAs in *Arabidopsis* and
296 *Capsella* respectively, indicating an expansion of the *COPIA95* TE family in *Capsella*
297 (Supplemental dataset 1). The prominent targeting of *COPIA95* in *Capsella* microspores
298 by Pol IV-dependent siRNAs made us address the question whether loss of Pol IV
299 function may cause increased expression and transposition of *COPIA95*. Indeed,
300 *COPIA95* was highly upregulated in *Cr nrpd1* microspores, but remained silenced in
301 microspores of *At nrpd1* (Figure 7C). To test whether increased expression caused
302 heritable transposition, we performed whole genome sequencing of five homozygous *Cr*
303 *nrpd1* mutants that were derived from homozygous *Cr nrpd1* parental plants. We mapped
304 genomic reads to *COPIA95* elements and found that one of the five tested mutants had
305 a two-fold increase of *COPIA95* elements (Figure 7D). We corroborated this result by
306 using TEPIID to identify *de novo* insertions (Stuart et al 2016) and also detected increased
307 insertions in the same mutant plant (Figure 7D). This result supports the idea that Pol IV
308 is required to prevent TE remobilization in *Capsella* and is, in particular, required to
309 silence *COPIA95*.

310 **Loss of Pol IV causes transcriptional changes in microspores**

311 To understand the cause for post-meiotic arrest of *Capsella* microspores, we compared
312 the transcriptome changes in *At* and *Cr nrpd1* microspores. We found a comparable
313 number of genes being upregulated (\log_2 fold-change >1 , $p < 0.05$) in *nrpd1* microspores
314 of both species; there were however about twice as many genes downregulated (\log_2
315 fold-change <-1 , $p < 0.05$) in *Cr nrpd1* microspores compared to *At nrpd1* (Supplemental
316 Figure 6A, B; Supplemental dataset 2). While there was no significant overlap between
317 downregulated genes in *Cr* and *At nrpd1* microspores (Supplemental Figure 6B), there
318 was a significant overlap of upregulated genes in *Cr* and *At nrpd1*, with a significant

319 enrichment for genes with functional roles in stimulus response, cell wall organization,
320 and defense responses (Supplemental Figure 6C).

321 We tested whether deregulated genes in *Cr* and *At nrpd1* microspores were targeted by
322 21/22-nt or 24-nt siRNAs. We found a significant overlap between upregulated genes and
323 downregulated genes with genes losing 21/22-nt and 24-nt siRNAs in *Cr nrpd1* (Figure
324 8A, Supplemental dataset 3). In contrast, in *At nrpd1* only downregulated genes
325 significantly overlapped with genes losing 21/22-nt and 24-nt siRNAs (Supplemental
326 Figure 6D, Supplemental dataset 4). Upregulated genes losing 21/22-nt or 24-nt siRNAs
327 in *Cr nrpd1* had functional roles in proteolysis and catabolic processes, cell killing, and
328 interspecies organismal interactions (Figure 8B). The distance of TEs to neighboring
329 genes was significantly shorter in *Capsella* compared to *Arabidopsis*, independently of
330 their direction of deregulation (Figure 8C; Wilcoxon test, $p<2e-15$). Nevertheless,
331 upregulated genes in *Capsella* had an even shorter distance to neighboring TE than non-
332 deregulated or downregulated genes, suggesting an impact of neighboring TEs on gene
333 expression in *Cr nrpd1* microspores. There was however no preference for *COP1A95*
334 among those TEs being close to deregulated genes ($p=1$, hypergeometric test).

335 Interestingly, we found that downregulated genes associated with loss of 21/22-nt and
336 24-nt siRNAs in *Cr nrpd1* were enriched for genes involved in pollination; among those
337 were known regulators of pollen tube growth like VANGUARD1 (VGD1), ANXUR2
338 (ANX2), CATION/H⁺ EXCHANGER 21 (CHX21), and JINGUBANG (JGB) (Figure 8D,
339 Supplemental Figure 7; Jiang et al., 2005; Boisson-Dernier et al., 2005; Lu et al., 2011;
340 Ju et al., 2016). We furthermore identified homologs of pollen receptor kinase encoding
341 genes *PRK2* and *PRK3* among downregulated genes losing 21/22-nt and 24-nt siRNAs
342 (Figure 8D, Supplemental Figure 7). While there was also a significant overlap of
343 downregulated genes in *At nrpd1* with genes losing siRNAs (Supplemental Figure 6D),
344 those genes were not enriched for genes involved in pollination (Supplemental Figure 6E)
345 and the aforementioned genes were not deregulated in *At nrpd1* (Figure 8D). The affected
346 pollen receptor kinases have partly redundant functions in pollen tube growth and
347 perception of female attractant peptides (Chang et al., 2013; Takeuchi and Higashiyama,
348 2016). Importantly, RNAi-mediated knockdown of *PiPRK1*, a PRK homologue Petunia,

349 causes microspore arrest (Lee et al., 1996), suggesting that reduced expression of PRKs
350 may contribute to the *Cr nrpd1* microspore arrest. All genes were highly induced in the
351 microspores to mature pollen transition (Figure 8E), suggesting that their expression is
352 required to ensure viable pollen formation, a hypothesis that remains to be tested.

353

354 **Discussion**

355 In this manuscript, we report that loss of Pol IV function in *Capsella rubella* causes arrest
356 of microspore development and a maternal effect on ovule and seed development,
357 strongly differing from the lack of obvious reproductive abnormalities of *nrpd1* mutants in
358 *Arabidopsis* (Mosher et al., 2009). Previous work revealed that mutations in NRPD1,
359 NRPE1 and RDR2 in *Brassica rapa* cause a maternal effect on seed development, while
360 no defect in pollen development was reported (Grover et al., 2018). The mutation in *B.*
361 *rapa* *NRPD1* was not a null allele; however, the mutation in *RDR2* completely abolished
362 production of 24-nt siRNAs (Grover et al., 2018), indicating that this mutant was a
363 functional null for *RDR2*. Since loss of *Cr NRPD1* caused a similar molecular effect as
364 mutations in *Arabidopsis* and *B. rapa* *NRPD1* (depletion of 24-nt siRNAs and CHH
365 methylation) (Wierzbicki et al., 2012; Panda et al., 2016; Grover et al., 2018) and that the
366 *Cr nrpd1* mutant could be complemented with the *Arabidopsis NRPD1* sequence, we
367 conclude that the molecular function of Pol IV is likely conserved between the three
368 species, but the targets differ. Interestingly, loss of Pol IV function in tomato also causes
369 sterility, but the cause for this phenotype remains to be explored (Gouil and Baulcombe,
370 2016). The microspore arrest in *Cr nrpd1* is possibly a consequence of TEs being in close
371 vicinity to either essential regulators of microspore development, like PRKs, or genes that
372 cause microspore arrest upon overexpression. The distance of TEs to neighboring genes
373 is substantially larger in *Arabidopsis* compared to *Capsella*, supporting this notion.

374 We observed a heritable remobilization of the COPIA95 element in progenies of *Cr nrpd1*
375 mutant, consistent with this element being preferentially targeted by Pol IV-generated
376 siRNAs in *Capsella* and strongly activated in *Cr nrpd1* microspores. Interestingly, in
377 *Arabidopsis*, the COPIA element ONSEN also undergoes transgenerational

378 retrotransposition in *nrpd1* after heat treatment and new *ONSEN* insertions differ between
379 siblings derived from a single plant (Ito et al., 2011). Since amplification of *COPIA* 95 was
380 only observed in one of the five tested *Cr nrpd1* progenies, it seems unlikely that the
381 consistently observed microspore arrest is connected to TE remobilization. Alternatively,
382 it is possible that only those microspores survive where TE remobilization did not occur,
383 or did occur at low frequency.

384 *Cr nrpd1* microspores were completely depleted for TE-derived siRNAs, including 21/22-
385 nt siRNAs, which are usually not associated with Pol IV (Xie et al., 2004; Zhai et al.,
386 2015a; Blevins et al., 2015). A similar depletion of 21/22-nt siRNAs (easiRNAs) was
387 previously reported in the mature pollen grain of *At nrpd1* mutants (Martinez et al., 2018;
388 Borges et al., 2018). The biogenesis of easiRNAs was suggested to be a consequence
389 of reduced heterochromatin formation in the vegetative cell and resulting TE activation
390 (Slotkin et al., 2009; Creasey et al., 2014). Based on genetic data Borges et al. (2018)
391 proposed that easiRNA biogenesis occurs earlier, during or early after meiosis. Our data
392 reveal that 21/22-nt TE-derived siRNAs are already present in the microspores and given
393 the similarity to meiocyte siRNAs (Huang et al., 2019), they are likely generated before or
394 during meiosis.

395 In rice and maize, highly abundant 21-nt phasiRNAs accumulate in premeiotic anthers
396 and 24-nt phasiRNAs are enriched in meiotic-stage anthers (Zhai et al., 2015b; Johnson
397 et al., 2009; Komiya et al., 2014). The 21-nt phasiRNAs were shown to be important for
398 male fertility in rice and disruption of 24-nt phasiRNA production yields conditional male
399 sterility in maize (Fan et al., 2016; Teng et al., 2018). Biogenesis of premeiotic and meiotic
400 phasiRNAs in maize seems to occur in the tapetum, rather than in meiocytes where they
401 accumulate (Zhai et al., 2015b). The production of 24-nt phasiRNAs depends on
402 *miR2275*, a pathway that is widely present in the eudicots, but missing in the
403 *Brassicaceae* (Xia et al., 2019), suggesting evolutionary divergence of the functional role
404 of phasiRNAs during pollen development. Cross-sections did not reveal obvious tapetal
405 defects in *Cr nrpd1*, indicating that microspore arrest in *Cr nrpd1* is not a consequence of
406 a tapetal defect.

407 The strong dependency of TE-derived siRNA accumulation on Pol IV suggests that Pol
408 IV transcripts are the precursors for all sizes of TE-derived siRNAs in microspores.
409 Previous work revealed that in the absence of DCL3, other DCL proteins (DCL1, DCL2,
410 and DCL4) are able to process Pol IV transcripts into 21- or 22-nt siRNAs (Gasciolli et al.,
411 2005; Henderson et al., 2006; Kasschau et al., 2007; Bond and Baulcombe, 2015). We
412 thus propose that before or during meiosis, Pol IV transcripts are targeted by other DCLs
413 than only DCL3, explaining why all sizes of Pol IV-dependent siRNAs derive from the
414 same TE loci.

415 In *Arabidopsis* siliques, a nuclear localized form of DCL4 was shown to target Pol IV
416 transcripts and generates 21-nt siRNAs (Pumplin et al., 2016). The abundance of those
417 21-nt Pol IV-derived siRNAs was nevertheless low, contrasting to the high abundance in
418 microspores. One possible explanation could be that the disruption of the nuclear
419 envelope during meiosis allows cytoplasmic DCLs to gain access to Pol IV/RDR2
420 transcripts. This implicates that meiosis is the trigger of Pol IV-dependent 21-24-nt siRNA
421 production, consistent with our genetic data. Not mutually exclusive with this scenario is
422 the possibility that 22-nt siRNAs produced during meiosis trigger secondary 21/22-nt
423 siRNA production in the mature pollen grain by targeting TE transcripts expressed in the
424 vegetative cell of pollen (Slotkin et al., 2009). This amplification of the signal by the
425 canonical post-transcriptional gene silencing (PTGS) pathway (Martinez de Alba et al.,
426 2013) should result in high abundant 21/22-nt siRNAs in mature pollen, which is in
427 agreement with published siRNA profiles of pollen (Martinez et al., 2018; Borges et al.,
428 2018).

429 We have shown that Pol IV-dependent 21/22-nt siRNAs are required to silence TEs in
430 microspores. This could be achieved by the non-canonical RdDM pathway involving
431 21/22-nt siRNAs (Cuerda-Gil and Slotkin, 2016); or, alternatively, by the PTGS pathway.
432 Levels of CHH methylation are low in meiocytes, but increase in microspores and in the
433 vegetative cell of pollen (Walker et al., 2018). Nevertheless, CHH methylation in
434 microspores is very low (Calarco et al., 2012), making it more likely that TE silencing in
435 microspores and later on in the vegetative cell is achieved by PTGS, consistent with the
436 high accumulation of 21/22-nt siRNAs in mature pollen.

437 Recent work from our and other groups revealed that disruption of NRPD1 suppresses
438 the hybridization barrier between plants of different ploidy grades (Martinez et al., 2018;
439 Satyaki and Gehring, 2019). However, while Martinez et al. (2018) did not find a
440 suppressive effect when using mutants in RdDM components such as *RDR2* and *NRPE1*,
441 Satyaki and Gehring (2019) found those mutants to suppress hybrid seed failure. The
442 difference between both studies lies in the use of tetraploid RdDM mutants by Satyaki
443 and Gehring (2019), while RdDM mutants introgressed into *omission of second division*
444 1 (*osd1*) were used by Martinez et al. (2018). Loss of *OSD1* suppresses the second
445 meiotic division, leading to unreduced gamete formation (d'Erfurth et al., 2009). Here, we
446 showed that *RDR2* is required for easiRNA biogenesis, suggesting that loss of easiRNAs
447 is not sufficient to suppress the triploid block induced by the *osd1* mutation. An important
448 difference between *osd1* and tetraploid plants is the ploidy of the genome at the beginning
449 of the meiosis, which is diploid and tetraploid, respectively. This fact can have a strong
450 impact, since tetraploid plants undergo DNA methylation changes leading to stable
451 epialleles (Mittelsten Scheid et al., 2003). Given that DNA methylation recruits Pol IV (Law
452 et al., 2013; Zhang et al., 2013) and our study points that easiRNAs are generated during
453 meiosis, it is possible that the requirement of RdDM activity for easiRNA formation and
454 ploidy barriers may be different depending of the initial ploidy of the plants. If true, the
455 signal establishing the triploid block depends on Pol IV but only indirectly on RdDM,
456 suggesting both pathways can be separated, as previously proposed in maize endosperm
457 (Erhard Jr. et al., 2013).

458 In summary, our study in *Capsella* uncovers a functional requirement of Pol IV in
459 microspores, emphasizing that Pol IV-dependent siRNA formation occurs earlier than
460 previously hypothesized (Slotkin et al., 2009). We show that Pol IV is generating the
461 precursors for 21-24-nt siRNAs, which may be a consequence of different DCLs being
462 able to access Pol IV transcripts during meiosis. Our study highlights the relevance of
463 investigating different plant models to gain novel insights into the molecular control of
464 developmental processes

465

466 **Methods**

467 **Plant growth and material**

468 Mutants alleles *nrpd1-3* (Salk_128428) and *dc3-1* (Salk_005512) have been previously
469 described (Pontier et al., 2005; Xie et al., 2004). For all experiments using *Arabidopsis*
470 *thaliana*, the Col-0 accession was used as wild type, while for *Capsella rubella*, accession
471 *Cr1GR1* was used.

472 Seeds of *Arabidopsis* and *Capsella* were surface sterilized in 5% commercial bleach and
473 0.01% Tween-20 for 10 min and washed three times in sterile ddH₂O. Seeds were sown
474 on ½ MS-medium (0.43% MS-salts, 0.8% Bacto Agar, 0.19% MES hydrate and 1%
475 Sucrose). After stratification for 2 days at 4°C, plates were transferred to a growth
476 chamber (16 h light / 8 h dark; 110 µmol/s/m²; 21°C; 70% humidity). After 10 days,
477 seedlings were transferred to soil and grown in a growth chamber (16 h light / 8 h dark;
478 110 µmol/s/m²; 21°C; 70% humidity). *Capsella* plants were grown in the growth chamber
479 at the same light-dark cycles, but at 18 °C and 60% humidity.

480 **Generation of plasmids and transgenic plants**

481 The web tool CRISPR-P (<http://cbi.hzau.edu.cn/cgi-bin/CRISPR>) was used to design the
482 sgRNAs for knocking out *Capsella NRPD1* (Carubv10019657m) (Lei et al., 2014).
483 Sequence information for the primers containing the two sgRNA sequences are listed in
484 Supplemental table 1. They were used for amplifying the fragment including Target1-
485 sgRNA-scaffold-U6-terminator-U6-29promoter-Target2 using plasmid DT1T2-PCR as
486 template (Wang et al., 2015). The amplified fragment was digested with *Bsal* and inserted
487 into pHEE401E containing an egg cell specific promoter driven Cas9 cassette as previous
488 described (Wang et al., 2015).

489 The pHEE401E-*NRPD1*-T1T2 construct was transformed into *Agrobacterium*
490 *tumefaciens* (GV3101) and bacteria containing the plasmid were used to transform
491 *Capsella rubella* accession *Cr1GR1* by floral dip (Clough and Bent, 1998). The genomic
492 sequence of *Arabidopsis NRPD1* with the stop codon was amplified from Col genomic
493 DNA and cloned into pDONR221 (Invitrogen) and after being confirmed by sequencing it

494 was inserted in pB7WG2 in which the CaMV35S promoter was replaced by the 1.6-kb
495 promoter sequence of *RPS5A* (Weijers et al., 2001).

496 **Microscopy**

497 *Capsella* inflorescences were harvested and fixed in 3:1 (Ethanol : acetic acid) solution.
498 Pollen were manually dissected from stage 12 and 13 anthers, and then stained with
499 DAPI (1 µg/ml) as previous described (Brownfield et al., 2015). The slides were observed
500 using a Zeiss Axio Scope.A1 and a Zeiss 7800 confocal microscope.

501 To generate sections, *Capsella* inflorescences were harvested and fixed in FAA solution
502 (50% Ethanol, 5% acetic acid, 4% formaldehyde) and embedded using the Leica
503 Historesin Embedding Kit (702218500). Three-micrometer sections were prepared using
504 a HM 355 S microtome (Microm) with glass knives. Sections were stained with 0.1%
505 toluidine blue for 1 min, washed five times with distilled water, air dried and then observed
506 using Zeiss Axio Scope.

507 **Microspore extraction**

508 The different pollen stages were extracted on a percoll gradient following previously
509 published procedures (Dupl'akova et al., 2016). The purity of each fraction was assessed
510 by Alexander and DAPI staining.

511 **RNA and small RNA sequencing**

512 RNA of *Arabidopsis* microspores was isolated using the TRIzol following the
513 manufacturer's protocol (Thermofischer: cat-15596018). Purified RNA was treated with
514 DNaseI (Thermofischer: cat-EN0521) and then loaded on a 15% TBE-Urea
515 polyacrylamide gel. RNA with a size of 15-27-nt was retrieved and eluted by crushing the
516 gel in PAGE elution buffer (1M Tris pH7.5, 2.5M NaOAc, 0.5M EDTA pH8) followed by
517 an overnight incubation and a new TRiZol extraction.

518 *Capsella* leaves were ground with liquid nitrogen, and 100 mg of fine powder from each
519 sample was used for RNA isolation. *Capsella* microspores were ground in a pre-cooled
520 mortar with Lysis/Binding Solution of the *mirVana*™ miRNA isolation kit. Both long RNAs

521 (>200-nt) and short RNAs (<200-nt) were isolated from leaves and microspores according
522 to the manufacturer's protocol (*mir*Vana™ miRNA Isolation Kit, AM1560). Size selection
523 of sRNAs was performed as described above.

524 For the RNA seq analysis, total RNA was treated with the Poly(A) mRNA Magnetic
525 Isolation Module kit (NEB #E7490). Libraries were prepared from the resulting mRNA with
526 the NEBNext® Ultra™ II kit (NEB #E7770S). sRNA seq libraries were generated with the
527 NEBNext® Multiplex Small RNA kit (NEB #E7300S). RNA-seq libraries and sRNA-seq
528 libraries were sequenced at the SciLife Laboratory (Uppsala, Sweden) and Novogene
529 (Hongkong, China) on a HiSeqX in 150-bp paired-end mode or a Illumina HiSeq2000 in
530 50-bp single-end mode, respectively.

531 **Bisulfite sequencing**

532 Leaves of 6-10 plants of *Capsella* wildtype and *nrpd1* mutants were pooled as one
533 replicate. Genomic DNA was extracted using the MagJET Plant Genomic DNA Kit
534 (K2761). The bisulfite conversion and library preparation were done as previously
535 described (Moreno-Romero et al., 2016). Libraries were sequenced at the SciLife
536 Laboratory (Uppsala, Sweden) on an Illumina HiSeq2000 in 125-bp paired-end mode.

537 **DNA sequencing**

538 Genomic DNA was isolated from leaves of one *Capsella* wild-type plant and five *pol iv*
539 mutants using the MagJET Plant Genomic DNA Kit (K2761). Libraries were generated
540 using the NEBNext® Ultra™ II DNA Library Prep Kit for Illumina® and sequenced at
541 Novogene (Hongkong, China) on an Illumina HiSeqX in 150-bp paired-end mode.

542 **Bioinformatic analysis**

543 For sRNA data, adapters were removed from the 50-bp long single-end sRNA reads in
544 each library. The resulting 18-30-bp long reads were mapped to the respective reference
545 genomes using bowtie (-v 0 --best). All reads mapping to chloroplast and mitochondria
546 and to structural noncoding RNAs (tRNAs, snRNAs, rRNAs, or snoRNAs) were removed.
547 Mapped reads from both replicates were pooled together, sorted in two categories (21/22-

548 nt and 24-nt long) and remapped to the same reference masked genome mentioned
549 above using ShortStack (--mismatches 0 --mmap f) (Johnson et al., 2016) in order to
550 improve the localization of sRNAs mapping to multiple genomic locations. We normalized
551 the alignments by converting coverage values to RPM values. TE-siRNAs were defined
552 as siRNAs that overlap with annotated TEs. TEs accumulating 20 or more reads in the
553 merged wild-type libraries were considered as TE producing siRNA loci. TEs losing
554 siRNAs in *nrpd1* were defined as those having less than 5% of reads left in *nrpd1*
555 compared to wild-type samples. To identify genes losing siRNAs in *nrpd1* microspores,
556 we determined siRNA coverage over the genomic loci plus 2kb up-and downstream
557 regions and calculated differences to wild-type microspores using the Bioconductor
558 RankProd Package (Hong et al 2006) (log2 fold change <-1, (percentage of false
559 prediction) pfp<0.05). For RNA analysis, for each replicate, reads were mapped to the
560 *Arabidopsis* and the *Capsella* reference genomes, using TopHat v2.1.0 (Trapnell et al,
561 2009) in single-end mode. Gene and TE expression was normalized to reads per kilobase
562 per million mapped reads (RPKM) using GFOLD (Feng et al, 2012). For Capsella the *C.*
563 *rubella* v1.0 annotated genome was used as reference (Slotte et al., 2013,
564 https://phytozome.jgi.doe.gov/pz/portal.html#!info?alias=Org_Crubella), which was also
565 used as reference in all *Capsella* analyses describe herein. For Arabidopsis the TAIR10
566 annotation was used. Expression level for each condition was calculated using the mean
567 of the expression values in both replicates. Differentially regulated genes and TEs across
568 the two replicates were detected using the rank product method, as implemented in the
569 Bioconductor RankProd Package (Hong et al 2006). For DNA methylation analysis, reads
570 of each pair were split in 50-bp-long fragments and mapped in single-end mode using
571 Bismark (Krueger and Andrews, 2011). Duplicated reads (aligning to the same genomic
572 position) were eliminated and methylation levels for each condition were calculated
573 averaging the replicates.

574 To estimate the number and identity of sRNA reads mapping to COPIA95 TEs in
575 *Capsella*, 21/22-nt and 24-nt sRNA reads were first mapped to a consensus reference
576 fasta file for *Arabidopsis* TEs available at Repbase
577 (<https://www.girinst.org/repbase/update/index.html>) (Jurka et al 2005) using bowtie (-v 2
578 -m 3 --best --strata). Reads mapping to COPIA95 TEs were remapped to the *C. rubella*

579 reference genome with ShortStack (–mismatches 0 –mmap f) (Johnson et al., 2016) and
580 normalized using coverage values of single copy genes.

581 New TE insertions in *Capsella rubella* were identified using TEPID (Stuart et al., 2016) in
582 pair-end mode based on the sequenced genomes of five *Cr pol iv* mutants and the
583 corresponding wild-type.

584 **Data availability**

585 The sequencing data generated in this study are available in the Gene Expression
586 Omnibus under accession number GSE129744. Supplemental Table 2 summarizes all
587 sequencing data generated in this study.

588

589 **Author Contributions and Acknowledgments**

590 ZW, NB, and CK performed the experimental design. ZW, NB, JY, and FB performed
591 experiments. GM advised on experimental work. RAM contributed experimental data. ZW,
592 NB, JSG, and CK analyzed the data. ZW, NB, JSG, and CK wrote the manuscript. All
593 authors read and commented on the manuscript.

594 We are grateful to Cecilia Wärdig for technical assistance. Sequencing was performed by
595 the SNP&SEQ Technology Platform, Science for Life Laboratory at Uppsala University,
596 a national infrastructure supported by the Swedish Research Council (VRFFI) and the
597 Knut and Alice Wallenberg Foundation. This research was supported by grants from the
598 Swedish Research Council VR and Formas (to CK), a grant from the Knut and Alice
599 Wallenberg Foundation (to CK), and support from the Göran Gustafsson Foundation for
600 Research in Natural Sciences and Medicine (to CK). Research in the Martienssen
601 laboratory is supported by the US National Institutes of Health (NIH) grant R01
602 GM067014, and by the Howard Hughes Medical Institute. The authors acknowledge
603 assistance from the Cold Spring Harbor Laboratory Shared Resources, which are funded
604 in part by the Cancer Center Support Grant (5PP30CA045508).

605 **References**

606 Bao, W., Kojima, K.K., and Kohany, O. (2015). Repbase Update, a database of
607 repetitive elements in eukaryotic genomes. *Mob DNA* 6: 11.

608 Baroux, C. and Autran, D. (2015). Chromatin dynamics during cellular differentiation in
609 the female reproductive lineage of flowering plants. *Plant J* 83: 160–176.

610 Berger, F. and Twell, D. (2011). Germline specification and function in plants. *Annu Rev*
611 *Plant Biol* 62: 461–484.

612 Blevins, T., Podicheti, R., Mishra, V., Marasco, M., Wang, J., Rusch, D., Tang, H., and
613 Pikaard, C.S. (2015). Identification of Pol IV and RDR2-dependent precursors of 24
614 nt siRNAs guiding de novo DNA methylation in *Arabidopsis*. *Elife* 4: e09591.

615 Boisson-Dernier, A., Roy, S., Krtsas, K., Grobeij, M.A., Jaciubek, M., Schroeder, J.I.,
616 Grossniklaus, U. (2009) Disruption of the pollen-expressed FERONIA homologs
617 ANXUR1 and ANXUR2 triggers pollen tube discharge. *Development* 136: 3279–
618 3288.

619 Bond, D.M. and Baulcombe, D.C. (2015). Epigenetic transitions leading to heritable,
620 RNA-mediated de novo silencing in *Arabidopsis thaliana*. *Proc Natl Acad Sci U S A*
621 112: 917–922.

622 Borg, M. and Berger, F. (2015). Chromatin remodelling during male gametophyte
623 development. *Plant J* 83: 177–188.

624 Borges, F. and Martienssen, R.A. (2013). Establishing epigenetic variation during
625 genome reprogramming. *RNA Biol* 10: 490–494.

626 Borges, F., Parent, J.S., van Ex, F., Wolff, P., Martinez, G., Kohler, C., and
627 Martienssen, R.A. (2018). Transposon-derived small RNAs triggered by miR845
628 mediate genome dosage response in *Arabidopsis*. *Nat Genet* 50: 186–192.

629 Brownfield, L., Yi, J., Jiang, H., Minina, E.A., Twell, D., and Köhler, C. (2015).
630 Organelles maintain spindle position in plant meiosis. *Nat. Commun.*

631 Calarco, J.P., Borges, F., Donoghue, M.T., Van Ex, F., Jullien, P.E., Lopes, T., Gardner,
632 R., Berger, F., Feijo, J.A., Becker, J.D., and Martienssen, R.A. (2012).
633 Reprogramming of DNA methylation in pollen guides epigenetic inheritance via
634 small RNA. *Cell* 151: 194–205.

635 Cao, X. and Jacobsen, S.E. (2002). Role of the *arabidopsis* DRM methyltransferases in
636 de novo DNA methylation and gene silencing. *Curr Biol* 12: 1138–1144.

637 Chang, F., Gu, Y., Ma, H., Yang, Z. (2013). AtPRK2 promotes ROP1 activation via
638 RopGEFs in the control of polarized pollen tube growth. *Mol Plant* 6: 1187-1201.

639 Clough, S.J. and Bent, A.F. (1998). Floral dip: a simplified method for Agrobacterium-
640 mediated transformation of *Arabidopsis thaliana*. *Plant J* 16: 735–743.

641 Creasey, K.M., Zhai, J., Borges, F., Van Ex, F., Regulski, M., Meyers, B.C., and
642 Martienssen, R.A. (2014). miRNAs trigger widespread epigenetically activated
643 siRNAs from transposons in *Arabidopsis*. *Nature* 508: 411–415.

644 Cuerda-Gil, D. and Slotkin, R.K. (2016). Corrigendum: Non-canonical RNA-directed
645 DNA methylation. *Nat Plants* 3: 16211.

646 d'Erfurth, I., Jolivet, S., Froger, N., Catrice, O., Novatchkova, M., and Mercier, R.
647 (2009). Turning Meiosis into Mitosis. *Plos Biol*. 7.

648 Dupl'akova, N., Dobrev, P.I., Renak, D., and Honys, D. (2016). Rapid separation of
649 *Arabidopsis* male gametophyte developmental stages using a Percoll gradient. *Nat
650 Protoc* 11: 1817–1832.

651 Erhard Jr., K.F., Parkinson, S.E., Gross, S.M., Barbour, J.E., Lim, J.P., and Hollick, J.B.
652 (2013). Maize RNA polymerase IV defines trans-generational epigenetic variation.
653 *Plant Cell* 25: 808–819.

654 Fan, Y. et al. (2016). PMS1T, producing phased small-interfering RNAs, regulates
655 photoperiod-sensitive male sterility in rice. *Proc Natl Acad Sci U S A* 113: 15144–
656 15149.

657 Feng J., Meyer C.A., Wang Q., Liu J.S., Shirley Liu X., and Zhang Y. (2012) GFOLD: a
658 generalized fold change for ranking differentially expressed genes from RNA-seq
659 data. *Bioinformatics* 28: 2782-2788.

660 Foxe, J.P., Slotte, T., Stahl, E.A., Neuffer, B., Hurka, H., and Wright, S.I. (2009). Recent
661 speciation associated with the evolution of selfing in *Capsella*. *Proc Natl Acad Sci U
662 S A* 106: 5241–5245.

663 Gasciolli, V., Mallory, A.C., Bartel, D.P., Vaucheret, H. (2005) Partially redundant
664 functions of *Arabidopsis* DICER-like enzymes and a role for DCL4 in producing
665 trans-acting siRNAs. *Curr Biol* 15: 1494-1500.

666 Grover, J.W., Kendall, T., Baten, A., Burgess, D., Freeling, M., King, G.J., and Mosher,
667 R.A. (2018). Maternal components of RNA-directed DNA methylation are required

668 for seed development in *Brassica rapa*. *Plant J* 94:575-582.

669 Gouil, Q., Baulcombe, D.C. (2016) DNA Methylation Signatures of the Plant
670 Chromomethyltransferases. *PLoS Genet* 12: e1006526.

671 Guo, Y.L., Bechsgaard, J.S., Slotte, T., Neuffer, B., Lascoux, M., Weigel, D., and
672 Schierup, M.H. (2009). Recent speciation of *Capsella rubella* from *Capsella*
673 *grandiflora*, associated with loss of self-incompatibility and an extreme bottleneck.
674 *Proc Natl Acad Sci U S A* 106: 5246–5251.

675 He, S., Vickers, M., Zhang, J., and Feng, X. (2019). Natural depletion of histone H1 in
676 sex cells causes DNA demethylation, heterochromatin decondensation and
677 transposon activation. *Elife* 8.

678 Henderson, I.R., Zhang, X., Lu, C., Johnson, L., Meyers, B.C., Green, P.J., and
679 Jacobsen, S.E. (2006). Dissecting *Arabidopsis thaliana* DICER function in small
680 RNA processing, gene silencing and DNA methylation patterning. *Nat Genet* 38:
681 721–725.

682 Herr, A.J., Jensen, M.B., Dalmay, T., and Baulcombe, D.C. (2005). RNA polymerase IV
683 directs silencing of endogenous DNA. *Science* 308: 118–120.

684 Hong, F., Breitling, R., McEntee, C.W., Wittner, B.S., Nemhauser, J.L., and Chory, J.
685 (2006). RankProd: a bioconductor package for detecting differentially expressed
686 genes in meta-analysis. *Bioinformatics* 22: 2825-2827.

687 Huang, J., Wang, C., Wang, H., Lu, P., Zheng, B., Ma, H., Copenhaver, G.P., and
688 Wang, Y. (2019). Meioocyte-specific and AtSPO11-1-dependent Small RNAs and
689 Their Association with Meiotic Gene Expression and Recombination. *Plant Cell*.

690 Ibarra, C.A. et al. (2012). Active DNA demethylation in plant companion cells reinforces
691 transposon methylation in gametes. *Science* 337: 1360–1364.

692 Ito H, Gaubert H, Bucher E, Mirouze M, Vaillant I, Paszkowski J. (2011) An siRNA
693 pathway prevents transgenerational retrotransposition in plants subjected to stress.
694 *Nature* 472: 115-119.

695 Jiang, L., Yang, S.L., Xie, L.F., Puah, C.S., Zhang, X.Q., Yang, W.C., Sundaresan, V.,
696 and Ye, D. (2005). VANGUARD1 encodes a pectin methylesterase that enhances
697 pollen tube growth in the *Arabidopsis* style and transmitting tract. *Plant Cell* 17:
698 584-596.

699 Johnson, C., Kasprzewska, A., Tennessen, K., Fernandes, J., Nan, G.L., Walbot, V.,
700 Sundaresan, V., Vance, V., and Bowman, L.H. (2009). Clusters and superclusters
701 of phased small RNAs in the developing inflorescence of rice. *Genome Res* 19:
702 1429–1440.

703 Johnson, N.R., Yeoh, J.M., Coruh, C., and Axtell, M.J. (2016). Improved Placement of
704 Multi-mapping Small RNAs. *G3* 6: 2103–2111.

705 Ju, Y., Guo, L., Cai, Q., Ma, F., Zhu, Q.Y., Zhang, Q., and Sodmergen (2016).
706 *Arabidopsis JINGUBANG Is a Negative Regulator of Pollen Germination That*
707 *Prevents Pollination in Moist Environments.* *Plant Cell* 28: 2131-2146.

708 Kasschau, K.D., Fahlgren, N., Chapman, E.J., Sullivan, C.M., Cumbie, J.S., Givan,
709 S.A., and Carrington, J.C. (2007). Genome-wide profiling and analysis of
710 *Arabidopsis* siRNAs. *PLoS Biol* 5: e57.

711 Kim, M.Y., Ono, A., Scholten, S., Kinoshita, T., Zilberman, D., Okamoto, T., and
712 Fischer, R.L. (2019). DNA demethylation by ROS1a in rice vegetative cells
713 promotes methylation in sperm. *Proc Natl Acad Sci U S A*.

714 Komiya, R., Ohyanagi, H., Niihama, M., Watanabe, T., Nakano, M., Kurata, N., and
715 Nonomura, K. (2014). Rice germline-specific Argonaute MEL1 protein binds to
716 phasiRNAs generated from more than 700 lincRNAs. *Plant J* 78: 385–397.

717 Krueger, F. and Andrews, S.R. (2011). Bismark: A flexible aligner and methylation caller
718 for Bisulfite-Seq applications. *Bioinformatics*.

719 de la Chaux, N., Tsuchimatsu, T., Shimizu, K.K., and Wagner, A. (2012). The
720 predominantly selfing plant *Arabidopsis thaliana* experienced a recent reduction in
721 transposable element abundance compared to its outcrossing relative *Arabidopsis*
722 *lyrata*. *Mob DNA* 3: 2.

723 Law, J.A., Du, J., Hale, C.J., Feng, S., Krajewski, K., Palanca, A.M., Strahl, B.D., Patel,
724 D.J., and Jacobsen, S.E. (2013). Polymerase IV occupancy at RNA-directed DNA
725 methylation sites requires SHH1. *Nature* 498: 385–389.

726 Lee H, Karunanandaa B, McCubbin A, Gilroy S, Kao T (1996). PRK1, a receptor-like
727 kinase of *Petunia inflata*, is essential for postmeiotic development of pollen. *Plant J*
728 9: 613-624.

729 Lei, Y., Lu, L., Liu, H.Y., Li, S., Xing, F., and Chen, L.L. (2014). CRISPR-P: a web tool

730 for synthetic single-guide RNA design of CRISPR-system in plants. *Mol Plant* 7:
731 1494–1496.

732 Lei, M., Zhang, H., Julian, R., Tang, K., Xie, S., Zhu, J.K. (2015) Regulatory link
733 between DNA methylation and active demethylation in *Arabidopsis*. *Proc Natl Acad
734 Sci U S A* 112: 3553-3557.

735 Li, S., Vandivier, L.E., Tu, B., Gao, L., Won, S.Y., Li, S., Zheng, B., Gregory, B.D., and
736 Chen, X. (2015). Detection of Pol IV/RDR2-dependent transcripts at the genomic
737 scale in *Arabidopsis* reveals features and regulation of siRNA biogenesis. *Genome
738 Res* 25: 235–245.

739 Lu, Y., Chanroj, S., Zulkifli, L., Johnson, M.A., Uozumi, N., Cheung, A., and Sze, H.
740 (2011). Pollen tubes lacking a pair of K⁺ transporters fail to target ovules in
741 *Arabidopsis*. *Plant Cell* 23: 81-93.

742 Martinez de Alba, A.E., Elvira-Matelot, E., and Vaucheret, H. (2013). Gene silencing in
743 plants: a diversity of pathways. *Biochim Biophys Acta* 1829: 1300–1308.

744 Martinez, G. et al. (2018). Paternal easiRNAs regulate parental genome dosage in
745 *Arabidopsis*. *Nat Genet* 50: 193–198.

746 Martinez, G., Panda, K., Kohler, C., and Slotkin, R.K. (2016). Silencing in sperm cells is
747 directed by RNA movement from the surrounding nurse cell. *Nat Plants* 2: 16030.

748 Maumus, F. and Quesneville, H. (2014). Ancestral repeats have shaped epigenome and
749 genome composition for millions of years in *Arabidopsis thaliana*. *Nat Commun* 5:
750 4104.

751 Mittelsten Scheid, O., Afsar, K., and Paszkowski, J. (2003). Formation of stable
752 epialleles and their paramutation-like interaction in tetraploid *Arabidopsis thaliana*.
753 *Nat. Genet.*

754 Moreno-Romero, J., Jiang, H., Santos-Gonzalez, J., and Kohler, C. (2016). Parental
755 epigenetic asymmetry of PRC2-mediated histone modifications in the *Arabidopsis*
756 endosperm. *EMBO J* 35: 1298–1311.

757 Mosher, R.A., Melnyk, C.W., Kelly, K.A., Dunn, R.M., Studholme, D.J., and Baulcombe,
758 D.C. (2009). Uniparental expression of PolIV-dependent siRNAs in developing
759 endosperm of *Arabidopsis*. *Nature* 460: 283–286.

760 Niu, X.M., Xu, Y.C., Li, Z.W., Bian, Y.T., Hou, X.H., Chen, J.F., Zou, Y.P., Jiang, J., Wu,

761 Q., Ge, S., Balasubramanian, S., and Guo, Y.L. (2019). Transposable elements
762 drive rapid phenotypic variation in *Capsella rubella*. *Proc Natl Acad Sci U S A* 116:
763 6908–6913.

764 Oliver, C., Santos, J.L., and Pradillo, M. (2016). Accurate chromosome segregation at
765 first meiotic division requires ago4, a protein involved in RNA-dependent DNA
766 methylation in *Arabidopsis thaliana*. *Genetics* 204: 543–553.

767 Onodera, Y., Haag, J.R., Ream, T., Costa Nunes, P., Pontes, O., and Pikaard, C.S.
768 (2005). Plant nuclear RNA polymerase IV mediates siRNA and DNA methylation-
769 dependent heterochromatin formation. *Cell* 120: 613–622.

770 Panda, K., Ji, L., Neumann, D.A., Daron, J., Schmitz, R.J., and Slotkin, R.K. (2016).
771 Full-length autonomous transposable elements are preferentially targeted by
772 expression-dependent forms of RNA-directed DNA methylation. *Genome Biol* 17:
773 170.

774 Pontier, D., Yahubyant, G., Vega, D., Bulski, A., Saez-Vasquez, J., Hakimi, M.A., Lerbs-
775 Mache, S., Colot, V., and Lagrange, T. (2005). Reinforcement of silencing at
776 transposons and highly repeated sequences requires the concerted action of two
777 distinct RNA polymerases IV in *Arabidopsis*. *Genes Dev* 19: 2030–2040.

778 Pumplin, N., Sarazin, A., Jullien, P.E., Bologna, N.G., Oberlin, S., and Voinnet, O.
779 (2016). DNA methylation influences the expression of DICER-LIKE4 isoforms,
780 which encode proteins of alternative localization and function. *Plant Cell* 28: 2786–
781 2804.

782 Satyaki, P.R. V and Gehring, M. (2019). Paternally acting canonical RNA-directed DNA
783 methylation pathway genes sensitize *Arabidopsis* endosperm to paternal genome
784 dosage. *Plant Cell* 31: 1563–1578.

785 Schmidt, A., Schmid, M.W., and Grossniklaus, U. (2015). Plant germline formation:
786 common concepts and developmental flexibility in sexual and asexual reproduction.
787 *Development* 142: 229–241.

788 Schoft, V.K., Chumak, N., Choi, Y., Hannon, M., Garcia-Aguilar, M., Machlicova, A.,
789 Slusarz, L., Mosiolek, M., Park, J.S., Park, G.T., Fischer, R.L., and Tamaru, H.
790 (2011). Function of the DEMETER DNA glycosylase in the *Arabidopsis thaliana*
791 male gametophyte. *Proc Natl Acad Sci U S A* 108: 8042–8047.

792 Singh, J., Mishra, V., Wang, F., Huang, H.Y., and Pikaard, C.S. (2019). Reaction
793 Mechanisms of Pol IV, RDR2, and DCL3 Drive RNA Channeling in the siRNA-
794 Directed DNA Methylation Pathway. *Mol Cell* 75: 576-589.

795 Slotkin, R.K., Vaughn, M., Borges, F., Tanurdzic, M., Becker, J.D., Feijo, J.A., and
796 Martienssen, R.A. (2009). Epigenetic reprogramming and small RNA silencing of
797 transposable elements in pollen. *Cell* 136: 461–472.

798 Slotte, T. et al. (2013). The *Capsella rubella* genome and the genomic consequences of
799 rapid mating system evolution. *Nat Genet* 45: 831–835.

800 Stuart, T., Eichten, S.R., Cahn, J., Karpievitch, Y. V, Borevitz, J.O., and Lister, R.
801 (2016). Population scale mapping of transposable element diversity reveals links to
802 gene regulation and epigenomic variation. *Elife* 5: e20777.

803 Takeuchi, H., Higashiyama, T. (2016). Tip-localized receptors control pollen tube growth
804 and LURE sensing in *Arabidopsis*. *Nature* 531: 245-248.

805 Tekleyohans, D.G., Nakel, T., and Gross-Hardt, R. (2017). Patterning the Female
806 Gametophyte of Flowering Plants. *Plant Physiol* 173: 122–129.

807 Teng, C., Zhang, H., Hammond, R., Huang, K., Meyers, B.C., and Walbot, V. (2018).
808 Dicer-like5 deficiency confers temperature-sensitive male sterility in maize. *bioRxiv*.

809 Trapnell, C., Pachter, L., and Salzberg, S.L. (2009). TopHat: discovering splice
810 junctions with RNA-Seq. *Bioinformatics* 25: 1105–1111.

811 Walker, J., Gao, H., Zhang, J., Aldridge, B., Vickers, M., Higgins, J.D., and Feng, X.
812 (2018). Sexual-lineage-specific DNA methylation regulates meiosis in *Arabidopsis*.
813 *Nat Genet* 50: 130–137.

814 Wang, Z.P., Xing, H.L., Dong, L., Zhang, H.Y., Han, C.Y., Wang, X.C., and Chen, Q.J.
815 (2015). Egg cell-specific promoter-controlled CRISPR/Cas9 efficiently generates
816 homozygous mutants for multiple target genes in *Arabidopsis* in a single
817 generation. *Genome Biol* 16: 144.

818 Weijers, D., Geldner, N., Offringa, R., and Jurgens, G. (2001). Seed development: Early
819 paternal gene activity in *Arabidopsis*. *Nature* 414: 709–710.

820 Wierzbicki, A.T., Cocklin, R., Mayampurath, A., Lister, R., Rowley, M.J., Gregory, B.D.,
821 Ecker, J.R., Tang, H., and Pikaard, C.S. (2012). Spatial and functional relationships
822 among Pol V-associated loci, Pol IV-dependent siRNAs, and cytosine methylation

823 in the *Arabidopsis* epigenome. *Genes Dev* 26: 1825–1836.

824 Wierzbicki, A.T., Ream, T.S., Haag, J.R., and Pikaard, C.S. (2009). RNA polymerase V
825 transcription guides ARGONAUTE4 to chromatin. *Nat Genet* 41: 630–634.

826 Villar, C., Erilova, A., Makarevich, G., Trösch, R., Köhler, C. (2009) Control of
827 PHERES1 imprinting in *Arabidopsis* by direct tandem repeats. *Mol Plant* 2: 654–
828 660.

829 Xia, R., Chen, C., Pokhrel, S., Ma, W., Huang, K., Patel, P., Wang, F., Xu, J., Liu, Z., Li,
830 J., and Meyers, B.C. (2019). 24-nt reproductive phasiRNAs are broadly present in
831 angiosperms. *Nat Commun* 10: 627.

832 Xie, Z., Johansen, L.K., Gustafson, A.M., Kasschau, K.D., Lellis, A.D., Zilberman, D.,
833 Jacobsen, S.E., and Carrington, J.C. (2004). Genetic and functional diversification
834 of small RNA pathways in plants. *PLoS Biol* 2: E104.

835 Xu, H., Knox, R.B., Taylor, P.E., and Singh, M.B. (1995). Bcp1, a gene required for
836 male fertility in *Arabidopsis*. *Proc Natl Acad Sci U S A* 92: 2106–2110.

837 Yang, D.L., Zhang, G., Tang, K., Li, J., Yang, L., Huang, H., Zhang, H., and Zhu, J.K.
838 (2016). Dicer-independent RNA-directed DNA methylation in *Arabidopsis*. *Cell Res*
839 26: 1264.

840 Zhai, J. et al. (2015a). A one precursor one siRNA model for Pol IV-dependent siRNA
841 biogenesis. *Cell* 163: 445–455.

842 Zhai, J., Zhang, H., Arikit, S., Huang, K., Nan, G.L., Walbot, V., and Meyers, B.C.
843 (2015b). Spatiotemporally dynamic, cell-type-dependent premeiotic and meiotic
844 phasiRNAs in maize anthers. *Proc Natl Acad Sci U S A* 112: 3146–3151.

845 Zhang, H. et al. (2013). DTF1 is a core component of RNA-directed DNA methylation
846 and may assist in the recruitment of Pol IV. *Proc Natl Acad Sci U S A* 110: 8290–
847 8295.

848 Zhang, H., Lang, Z., and Zhu, J.K. (2018). Dynamics and function of DNA methylation in
849 plants. *Nat Rev Mol Cell Biol* 19: 489–506.

850 Zhang, Y., McCormick, S. (2007). A distinct mechanism regulating a pollen-specific
851 guanine nucleotide exchange factor for the small GTPase Rop in *Arabidopsis*
852 *thaliana*. *Proc Natl Acad Sci U S A* 104: 18830–18835.

853 Zilberman, D., Cao, X., and Jacobsen, S.E. (2003). ARGONAUTE4 control of locus-

854 specific siRNA accumulation and DNA and histone methylation. *Science* (80-).
855 299: 716–719.

856

857 **Figure legends**

858 **Figure 1. Disruption of *NRPD1* in *Capsella* impairs 24-nt siRNA formation and**

859 **RdDM.**

860 (A) Deleted genomic region in *Capsella NRPD1* at 1634 – 2108 bp (genomic sequence).
861 Target 1 (T1) and target (T2) sequences of Crispr/Cas9 are indicated.
862 (B) Profile of TE-derived siRNAs in *Capsella* wild-type (wt) and *nrpd1* leaves.
863 (C) DNA methylation levels at TEs in *Capsella* wt and *nrpd1* leaves.

864

865 **Figure 2. Loss of *NRPD1* in *Capsella* affects female fertility and causes a reduction**

866 **of seed size.**

867 (A) Total seed numbers per siliques in wild-type (wt) (11 siliques) and *Cr nrpd1* mutant (24
868 siliques) plants. ***p <0.001 (Student's t-test). (B-D) Siliques at 2 days after pollination
869 (DAP) from (B) wt × wt, (C) *nrpd1*/+ × wt, (D) *nrpd1* × wt crosses. Bar (B-D): 1mm.
870 Asterisks mark unfertilized ovules. (E) Fertilization frequency in indicated crosses. 16
871 siliques per cross combination were analyzed. ** p < 0.01 (Student's t-test). (F-H) Ovules
872 at 2 days after emasculation of (F) wt, (G) *nrpd1*/+, (H) *nrpd1* plants. Bar (F-H): 20 µm.
873 (I-K) Seeds harvested from (I) wt × wt, (J) *nrpd1*/+ × wt, (K) *nrpd1* × wt crosses. Bar (I-K):
874 1mm. (L) Seed size of mature seeds derived from wt × wt (n=120), *nrpd1*/+ × wt (n=149),
875 *nrpd1* × wt (n=64) *** p < 0.001 (Student's t-test). n.s, not significant.

876

877 **Figure 3. *Cr nrpd1* pollen arrest at the microspore stage.**

878 (A-D) Bright field and (E-H) corresponding DAPI staining of manually dissected pollen
879 from anthers at stage 12/13. Pollen of wt (A and E), *Cr nrpd1* homozygotes (B and F), *Cr*
880 *nrpd1* heterozygotes (C and G), and a complemented line (D and H). Bar (A-H): 50 µm.
881 Confocal images of DAPI stained pollen of wild type (wt) (I), *Cr nrpd1* homozygotes (J),
882 and *Cr nrpd1* heterozygotes (K). Bar (I-K): 5 µm. (L) Percentage of mature pollen (MP) in
883 anthers dissected at stage 12/13 from wt, *Cr nrpd1* homozygotes (*nrpd1*), *Cr nrpd1*
884 heterozygotes (*nrpd1*/+) and a complemented line (compl.). Numbers of pollen counted

885 in each genotype were shown on top of the bars. Microsporangia cross-sections stained
886 with Toluidine Blue at anther stage 8 (M and O), 11 (Q and S), and 12 (R and T) of wt (M,
887 Q and R) and *Cr nrpd1* (O, S and T). Bar (M,O,Q-T): 50 μ m. Insets in (M) and (O) are
888 shown enlarged in (N) (P), respectively. Bar (N and P): 50 μ m. wt, wild type.

889
890 **Figure 4. Pol IV is required for 21-24-nt siRNAs in *Capsella* microspores.**
891 (A) Profile of TE- derived siRNAs in *Capsella* wt and *nrpd1* microspores. (B) Abundance
892 of TE-derived Cr NRPD1-dependent 21-22-nt siRNAs and 24-nt siRNAs in *Capsella*
893 microspores. Values are indicated as the log10 of the average RPM of both libraries.
894 Each dot represents one TE for a total of 5455 TEs. The correlation has been tested by
895 a Spearman test (correlation coefficient 0.6872). (C) Loss of 21/22-nt and 24-nt siRNAs
896 at TEs associates with increased transcript level of TEs in *Cr nrpd1* microspores.
897 Increasing accumulation of siRNAs over TEs is plotted from low to high levels of
898 accumulation. Only TEs with siRNAs more in wt than in *Cr nrpd1* are represented.
899 Differences between first and last categories are significant ($P = 3.4\text{e-}13$ and $1.4\text{e-}9$,
900 respectively, Wilcoxon test). (D) sRNA profile of TE-derived siRNAs from *Arabidopsis* wt
901 and *nrpd1* microspores.

902
903 **Figure 5. Meiocytes, microspores and mature pollen grain accumulate overlapping**
904 **sets of siRNAs.**

905 (A) TE-derived siRNA distribution in *Arabidopsis* meiocytes of the indicated genetic
906 background (data from Huang et al., 2019). (B) TE-derived siRNA distribution in
907 *Arabidopsis* pollen grains of the indicated genetic background. (C) Upset plot showing the
908 overlap of TEs accumulating 21/22-nt siRNAs or 24-nt siRNAs in *Arabidopsis*
909 microspores and meiocytes (data from Huang et al., 2019). (D) Upset plot showing the
910 overlap of TEs accumulating 21/22-nt siRNAs or 24-nt siRNAs in *Arabidopsis*
911 microspores and mature pollen grain (MPG) (data from Martinez et al., 2018).

912
913 **Figure 6. Pol IV/RDR2 generate templates for 21-24-nt siRNAs.**
914 (A) Loss of Pol IV-dependent 21/22-nt easiRNAs associates with increased transcript
915 levels of TEs in *Arabidopsis* microspores. Increasing accumulation of siRNAs over TEs is

916 plotted from low to high levels of accumulation. In both plots, siRNAs levels at TEs in wt
917 increase from left to right in quantiles. Differences between first and last categories are
918 significant ($p = 2.6\text{e-}10$ and $1.5\text{ e-}14$, respectively, Wilcoxon test). (B) Abundance of At
919 NRPD1-dependent 21-22-nt siRNAs and 24-nt siRNAs at TEs in *Arabidopsis* microspores.
920 Values are indicated as \log_{10} of the average reads per million (RPM) of both libraries.
921 Each dot represents one TE for a total of 1504 TEs. The correlation has been tested by
922 a Spearman test (correlation coefficient 0.7686). (C) Plots showing the distribution of the
923 ratio of the number of reads mapped against the positive strand to the total number of
924 mapped reads. Left plots shows analysis for 21/22-nt reads, right plot for 24-nt reads. (D)
925 TE-derived siRNA distribution in inflorescences of *rdr2* (left panel; data from Zhai et al.,
926 2015) and *rdr6* (right panel; data from Panda et al., 2016).
927 (E) Average total 21/22-nt or 24-nt reads mapping against TEs in wt or *dcl3* libraries (data
928 from Li et al., 2015). Reads were normalized to show RPM values. (F) Average total
929 21/22-nt reads mapping against miRNAs in wt or *dcl3* libraries (data from Li et al., 2015).
930 Reads were normalized to show RPM values.

931

932 **Figure 7. COPIA95-siRNAs are highly enriched in *Capsella* microspores.**

933 (A) Upset plots of TE families accumulating Pol IV-dependent 21/22-nt and 24-nt siRNAs
934 in *Arabidopsis* (*At*) and *Capsella* (*Cr*). (B) Proportions of Pol IV-dependent 21/22-nt and
935 24-nt siRNAs accumulating at specific TE consensus sequences in relation to all TE-
936 siRNAs. Reads mapping to COPIA95 long-terminal repeats (LTR) and internal (I)
937 sequences are highlighted in red and yellow, respectively. (C) Log2 expression fold
938 change of mRNAs for COPIA95 elements in *nrpd1* mutant microspores of *Arabidopsis*
939 and *Capsella* compared to the corresponding wild type. ** $p < 0.01$ (Student's t-test). (D)
940 Relative number of COPIA95 insertions (left panel) and total TE insertions (right panel)
941 compared to the corresponding wild-type control in five progenies of homozygous *Cr*
942 *nrpd1*.

943

944 **Figure 8. Deregulated genes differ in *Arabidopsis* and *Capsella nrpd1* mutant
945 microspores.**

946 (A) Venn diagrams showing overlap of deregulated genes ($|\log_2 \text{fold change}| > 1, p < 0.05$)
947 in *nrpd1* microspores of *Capsella* and genes losing 21/22-nt and 24-nt siRNAs at 2kb up-
948 and downstream and gene body ($\log_2 \text{fold change} < -1, p < 0.05$) in *Capsella nrpd1*
949 microspores. (B) Enriched gene ontologies (GOs) for biological processes of intersected
950 genes losing siRNAs and deregulated genes in *Capsella nrpd1* microspores. Top 5 GOs
951 of each analysis are shown. (C) Distance of *Arabidopsis* and *Capsella* genes to closest
952 TEs. All: all genes, up: significantly upregulated genes, down: significantly downregulated
953 genes. * $p < 0.05$, ** $p < 0.01$, *** $p < 0.001$, n.s, not significant. (Statistical analysis:
954 Wilcoxon test). (D) Log₂ expression fold change of *VGD1*, *PRK2*, *PRK3*, *CHX21*, *JGB*
955 and *ANX2* genes in *nrpd1* microspores compared to wild type (wt) in *Capsella* (*Cr*) and
956 *Arabidopsis* (*At*). (E) mRNA levels of *VGD1*, *PRK2*, *PRK3*, *CHX21*, *JGB* and *ANX2* in
957 *Arabidopsis* wild-type meiocytes, microspores and mature pollen grain (MPG). We added
958 plus 1 to all values to avoid negative log₁₀ values.

959

960 **Supplemental Figure legends**

961 **Supplemental Figure 1. Meiosis is not affected in *Capsella nrpd1*. Supports Figure 962 2.**

963 Meiosis in *Capsella* wild-type (A - H) and *nrpd1* (I - P) plants. A and I, pachytene. B and
964 J, diakinesis. C and K, metaphase I. D and L, telophase I. E and M, prophase II. F and
965 N, metaphase II. G and O, anaphase II. H and P, telophase II. Bar: 5 μm .

966

967 **Supplemental Figure 2. Normal tetrad formation in *Capsella* wild type (A) and *pol 968 iv* (B). Supports Figure 2.**

969 Shown are whole mount confocal images. Bar: 20 μm .

970

971 **Supplemental Figure 3. Average purity of *Capsella* and *Arabidopsis* microspore 972 extractions. Supports Figure 4.**

973 Microspore extractions of *Capsella* (A) and *Arabidopsis* (B) were tested by DAPI
974 staining and the B2 and B1 fractions were selected as the fractions containing the
975 highest proportion of microspores in *Capsella* and *Arabidopsis*, respectively. Shown is

976 the average percentage of four and eight independent extractions in *Capsella* and
977 *Arabidopsis*, respectively. Error bars show standard deviation.

978

979 **Supplemental Figure 4. Profile of total sRNAs in *Capsella* (A) and *Arabidopsis* (B)**
980 **microspores. Supports Figure 4.**

981

982 **Supplemental Figure 5. Example of four loci producing Pol IV-dependent siRNAs**
983 **in *Arabidopsis*. Supports Figure 7.**

984 Bars represent normalized reads. The color indicates the length of the analyzed reads:
985 red 24-nt, blue 22-nt, and green 21-nt. The DNA strand is indicated by the (+) or (-). TE
986 sequences are represented in yellow.

987

988 **Supplemental Figure 6. Deregulated genes in *Arabidopsis nrpd1* mutant**
989 **microspores. Supports Figure 8.**

990 (A) Venn diagram showing overlap of upregulated genes in *nrpd1* microspores of
991 *Capsella* and *Arabidopsis*. Significance was determined by a hypergeometric test. (B)
992 Venn diagram showing overlap of downregulated genes in *nrpd1* microspores of *Capsella*
993 and *Arabidopsis*. Significance was determined by a hypergeometric test. (C) Enriched
994 gene ontologies (GOs) for biological processes of upregulated genes shared in
995 *Arabidopsis* and *Capsella nrpd1* microspores. Top 5 GOs are shown. (D) Venn diagrams
996 showing overlap of deregulated genes ($|\log_2 \text{fold change}| > 1$, $p < 0.05$) in *nrpd1*
997 microspores of *Arabidopsis* and genes losing 21/22-nt and 24-nt siRNAs at 2kb up-and
998 downstream and gene body ($\log_2 \text{fold change} < -1$, $p < 0.05$) in *Arabidopsis nrpd1*
999 microspores. Significance was determined by a hypergeometric test.

1000 **Supplemental Figure 7. Representative pollen developmental genes accumulating**
1001 **21/22-nt and 24-nt siRNAs in *Capsella* microspores.**

1002

1003 **Supplemental datasets**

1004 **Supplemental dataset 1. COPIA95 elements accumulating Pol IV-dependent**
1005 **siRNAs in *Capsella* and *Arabidopsis*.**

1006 **Supplemental dataset 2. Up-and downregulated genes in *Arabidopsis* and**
1007 ***Capsella* microspores.**

1008 **Supplemental dataset 3. Up-and downregulated genes in *Capsella* microspores**
1009 **overlapping with regions losing 21/22-or 24-nt siRNAs in *Cr nrpd1* microspores.**

1010 **Supplemental dataset 4. Up-and downregulated genes in *Arabidopsis***
1011 **microspores overlapping with regions losing 21/22-or 24-nt siRNAs in *At nrpd1***
1012 **microspores.**

1013

1014 **Supplemental table 1. Primer list.**

1015 **Supplemental table 2. Quality of sequencing samples.**

1016

1017

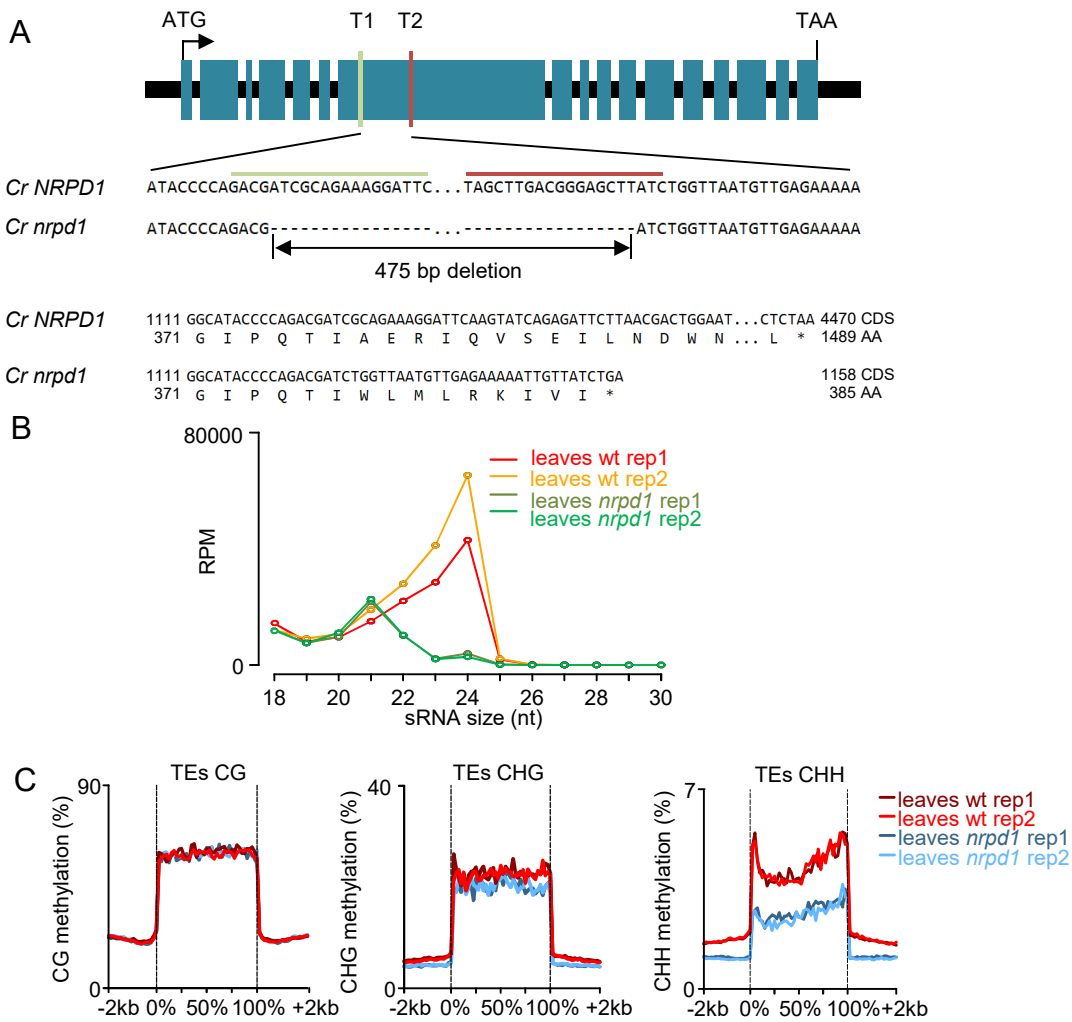


Figure 1. Disruption *NRPD1* in *Capsella* impairs 24-nt siRNA formation and RdDM.
 (A) Deleted genomic region in *Capsella NRPD1* at 1634 – 2108 bp (genomic sequence). Target 1 (T1) and target (T2) sequences of Crispr/Cas9 are indicated.
 (B) Profile of TE-derived sRNAs in *Capsella* wild-type (wt) and *nrpd1* leaves.
 (C) DNA methylation levels at TEs in *Capsella* wt and *nrpd1* leaves.

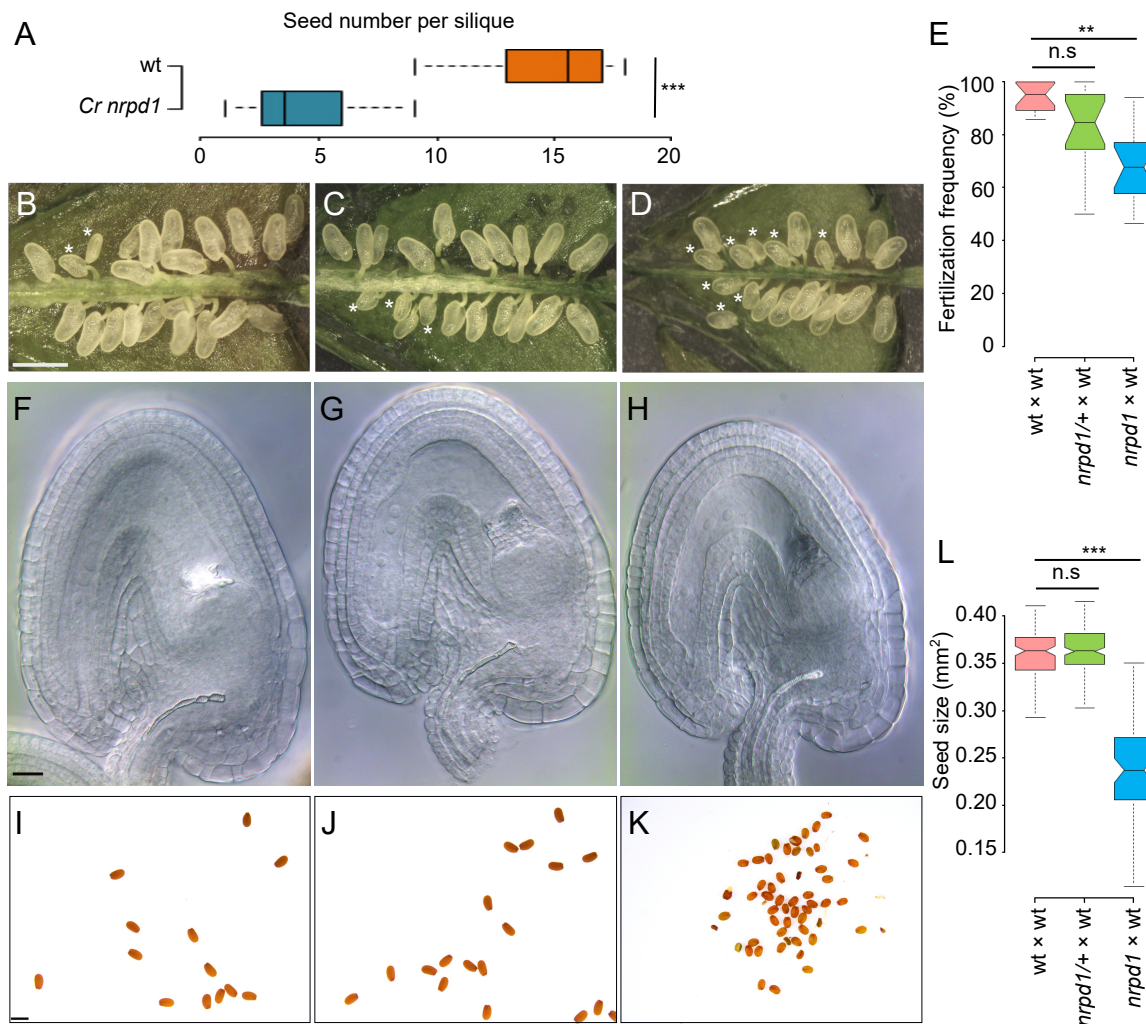


Figure 2. Loss of *NRPD1* in *Capsella* affects female fertility and causes a reduction of seed size.

(A) Total seed numbers per silique in wt (11 siliques) and *Cr nrpd1* mutant (24 siliques) plants. *** p-value < 0.001 (Student t-test). Siliques at 2 days after pollination (DAP) from (B) wt x wt, (C) *nrpd1*/+ x wt, (D) *nrpd1* x wt crosses. Bar (B-D): 1mm. Asterisks mark unfertilized ovules.

(E) Fertilization frequency in indicated crosses. 16 siliques per cross combination were analyzed. ** p-value < 0.01 (Student t-test). Ovules at 2 days after emasculation of (F) wt, (G) *nrpd1*/+, (H) *nrpd1* plants. Bar (F-H): 20 μ m. Seeds harvested from (I) wt x wt, (J) *nrpd1*/+ x wt, (K) *nrpd1* x wt crosses. Bar (I-K): 1mm. (L) Seed size of mature seeds derived from wt x wt (n=120), *nrpd1*/+ x wt (n=149), *nrpd1* x wt (n=64). *** p-value < 0.001 (Student t-test). n.s., not significant.

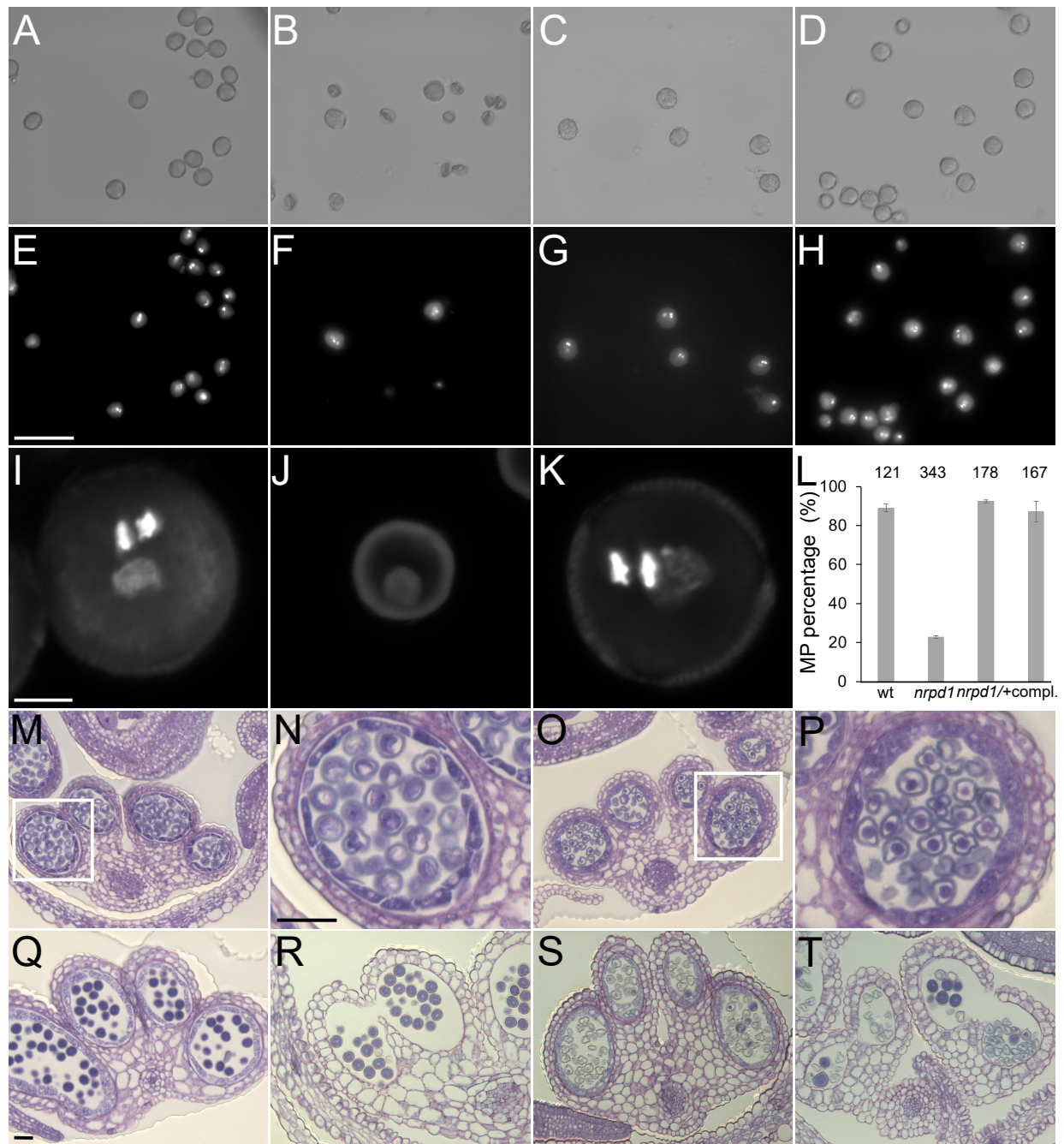


Figure 3. *Cr nrpd1* pollen arrest at the microspore stage.

(A - D) Bright field and (E – H) corresponding DAPI staining of manually dissected pollen from anthers at stage 12/13. Pollen of wild type (wt) (A and E), *Cr nrpd1* homozygotes (B and F), *Cr nrpd1* heterozygotes (C and G), and a complemented line (D and H). Bar (A-H): 50 μ m. Confocal images of DAPI stained pollen of wt (I), *Cr nrpd1* homozygotes (J), and *Cr nrpd1* heterozygotes (K). Bar (I-K): 5 μ m. (L) Percentage of mature pollen (MP) in anthers dissected at stage 12/13 from wt, *Cr nrpd1* homozygotes (*nrpd1*), *Cr nrpd1* heterozygotes (*nrpd1/+*) and a complemented line (compl.), numbers of pollen counted in each genotype were shown on top of the bars accordingly. Microsporangia cross-sections stained with Toluidine Blue at anther stage 8 (M and O), 11 (Q and S), and 12 (R and T) of wt (M, Q and R) and *Cr nrpd1* (O, S and T). Bar (M,O, Q-T): 50 μ m. Insets in (M) and (O) are shown enlarged in (N) (P), respectively. Bar (N and P): 50 μ m. wt, wild type.

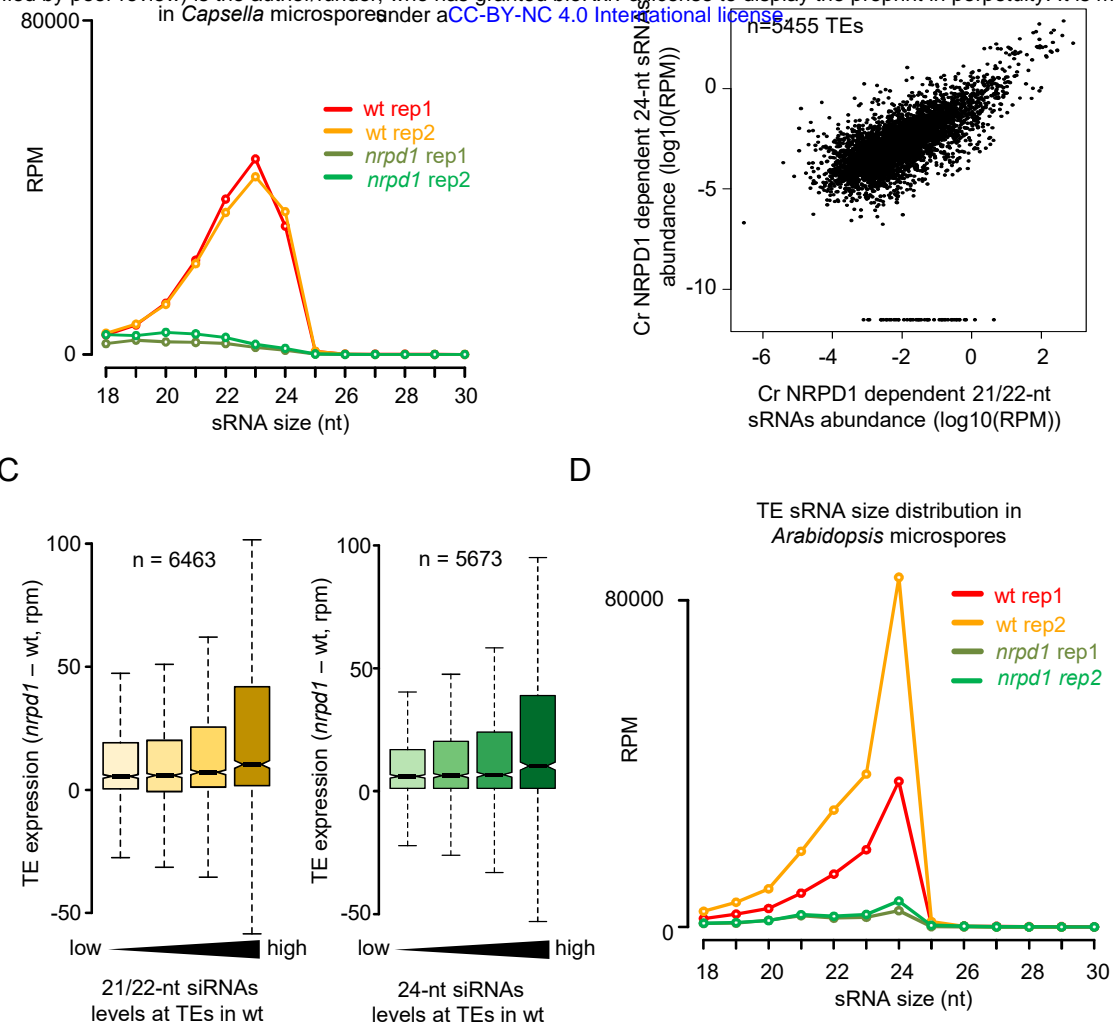


Figure 4. NRPD1 is required for 21-24-nt siRNAs in *Capsella* microspores.

(A) Profile of TE-derived siRNAs in *Capsella* wild-type (wt) and *nRPD1* microspores.

(B) Abundance of TE-derived Cr NRPD1-dependent 21/22-nt siRNAs and 24-nt siRNAs in *Capsella* microspores. Values are indicated as the log10 of the average RPM of both libraries. Each dot represents one TE for a total of 5455 TEs. The correlation has been tested by a Spearman test (correlation coefficient 0.6872).

(C) Loss of 21/22-nt and 24-nt siRNAs at TEs associates with increased transcript level of TEs in *Cr nRPD1* microspores. Increasing accumulation of siRNAs over TEs is plotted from low to high levels of accumulation. Only TEs with siRNAs more in wt than in *Cr nRPD1* are represented. Differences between first and last categories are significant ($p = 3.4\text{e-}13$ and $1.4\text{e-}9$, respectively, Wilcoxon test).

(D) sRNA profile of TE-derived sRNAs from *Arabidopsis* wt and *nRPD1* microspores.

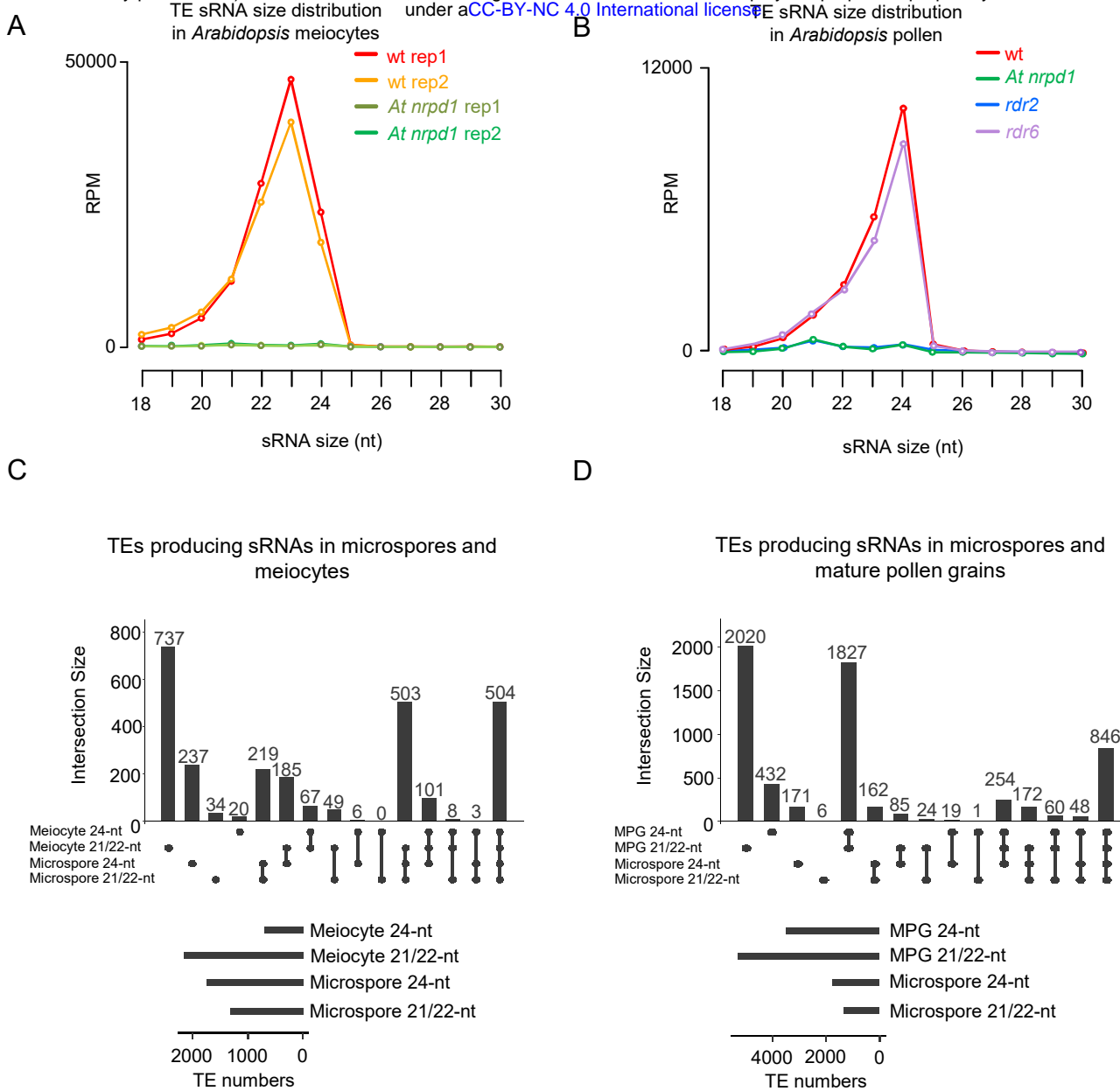


Figure 5. Meiocytes, microspores and mature pollen grain accumulate overlapping sets of siRNAs.

- (A) TE-derived siRNA distribution in *Arabidopsis* meiocytes of the indicated genetic background (data from Huang et al., 2019).
- (B) TE-derived siRNA distribution in *Arabidopsis* pollen grains of the indicated genetic background.
- (C) Upset plot showing the overlap of TEs accumulating 21/22-nt siRNAs or 24-nt siRNAs in *Arabidopsis* microspores and meiocytes (data from Huang et al., 2019).
- (D) Upset plot showing the overlap of TEs accumulating 21/22-nt siRNAs or 24-nt siRNAs in *Arabidopsis* microspores and mature pollen grain (MPG) (data from Martinez et al., 2018).

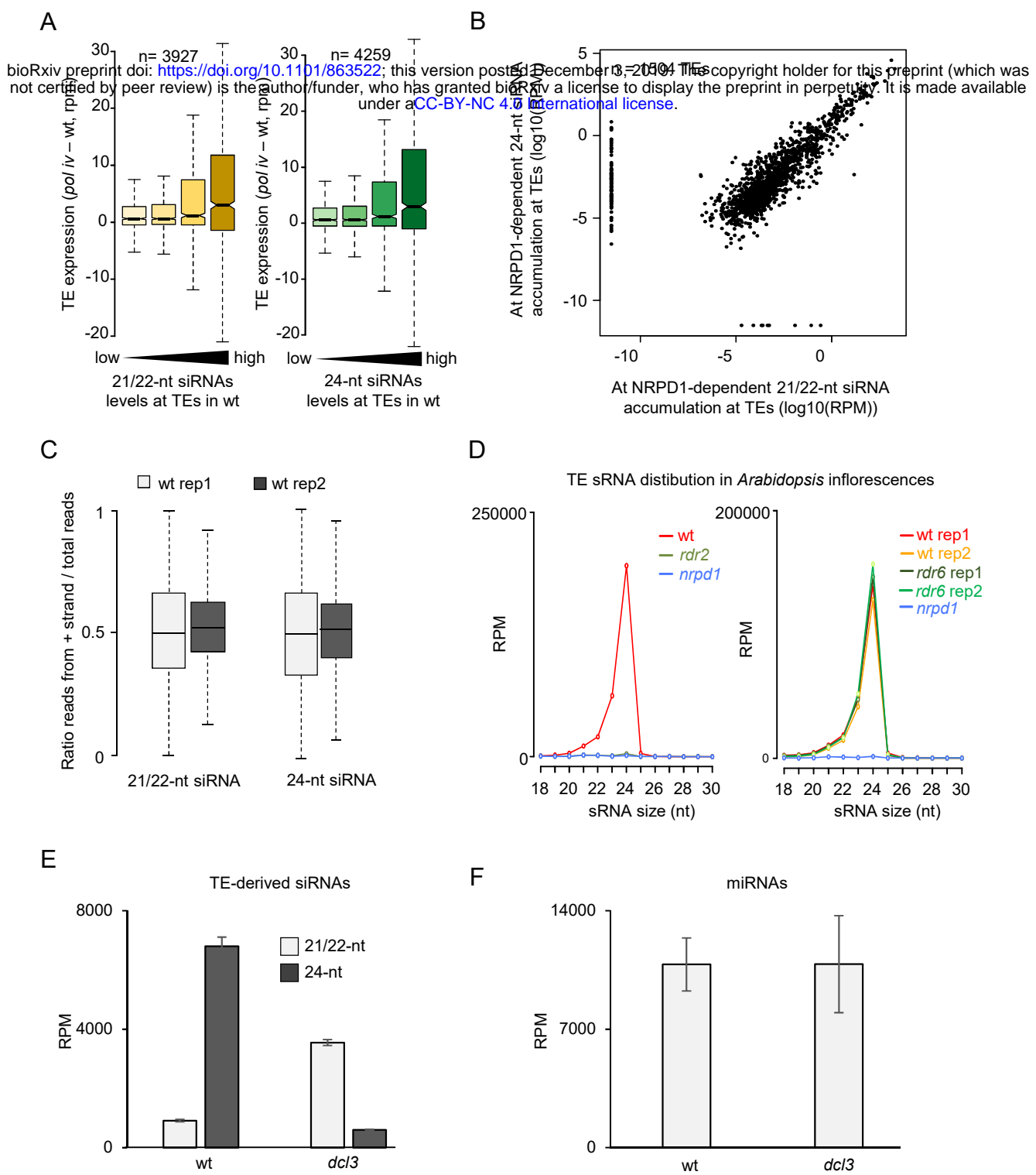


Figure 6. Pol IV/RDR2 generate templates for 21-24-nt siRNAs.

(A) Loss of At NRPD1 dependent 21/22-nt easiRNAs associates with increased transcript levels of TEs in *Arabidopsis* microspores. Increasing accumulation of siRNAs over TEs is plotted from low to high levels of accumulation. In both plots, siRNAs levels at TEs in wt increase from left to right in quantiles. Differences between first and last categories are significant ($p = 2.6e-10$ and $1.5e-14$, respectively, Wilcoxon test).

(B) Abundance of At NRPD1-dependent 21/22-nt siRNAs and 24-nt siRNAs at TEs in *Arabidopsis* microspores. Values are indicated as \log_{10} of the average reads per million (RPM) of both libraries. Each dot represents one TE for a total of 1504 TEs. The correlation has been tested by a Spearman test (correlation coefficient 0.7686).

(C) Plots showing the distribution of the ratio of the number of reads mapped against the positive strand to the total number of mapped reads. Left plots shows analysis for 21/22-nt reads, right plot for 24-nt reads.

(D) TE-derived siRNA distribution in inflorescences of *rdr2* (left panel; data from Zhai et al., 2015) and *rdr6* (right panel; data from Panda et al., 2016).

(E) Average total 21/22-nt or 24-nt reads mapping against TEs in wt or *dc1/3* libraries (data from Li et al., 2015). Reads were normalized to show RPM values.

(F) Average total 21/22-nt reads mapping against miRNAs in wt or *dc1/3* libraries (data from Li et al., 2015). Reads were normalized to show RPM values.

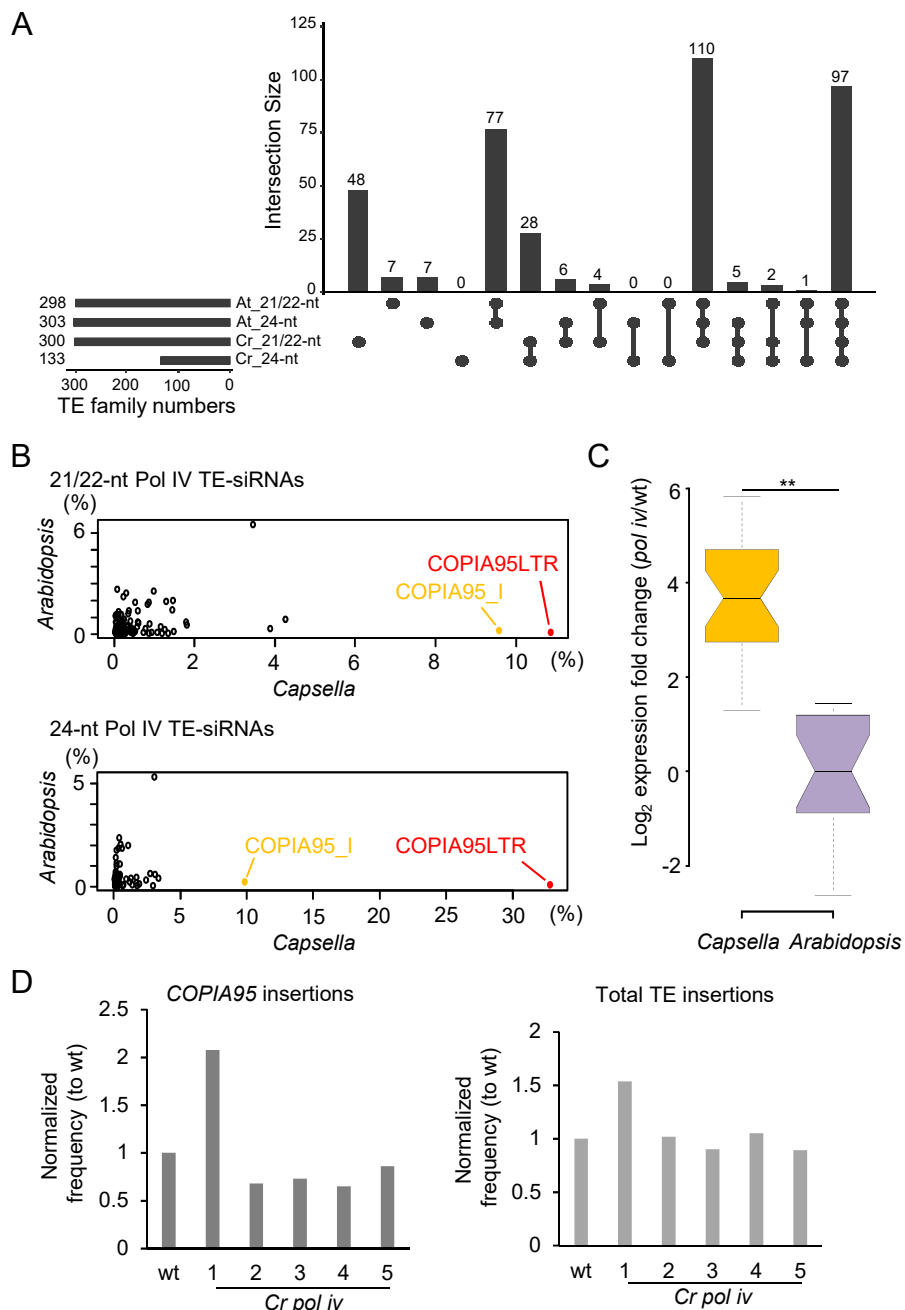


Figure 7. COPIA95-siRNAs are highly enriched in *Capsella* microspores.

(A) Upset plots of TE families accumulating Pol IV-dependent 21/22-nt and 24-nt siRNAs in *Arabidopsis* (At) and *Capsella* (Cr).

(B) Proportions of Pol IV-dependent 21/22-nt and 24-nt siRNAs accumulating at specific TE consensus sequences in relation to all TE-siRNAs. Reads mapping to *COPIA95* long-terminal repeats (LTR) and internal (I) sequences are highlighted in red and yellow, respectively.

(C) Log₂ expression fold change of mRNAs for *COPIA95* elements in *nrpd1* mutant microspores of *Arabidopsis* and *Capsella* compared to the corresponding wild type.

** p < 0.01 (Student's t-test).

(D) Relative number of *COPIA95* insertions (left panel) and total TE insertions (right panel) compared to the corresponding wild-type control in five progenies of homozygous *Cr nrpd1*.

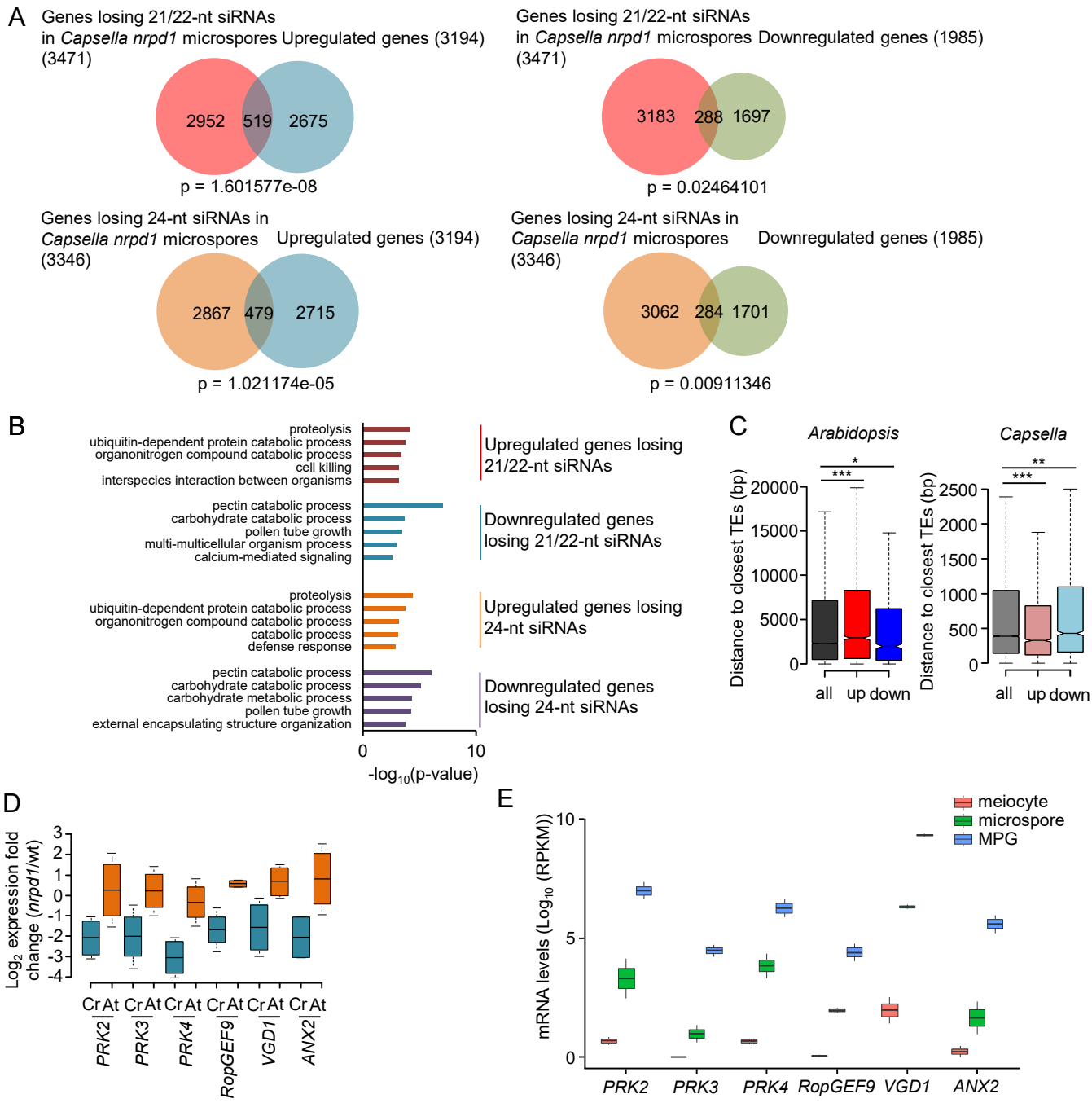


Figure 8. Deregulated genes differ in *Arabidopsis* and *Capsella nRPD1* mutant microspores.

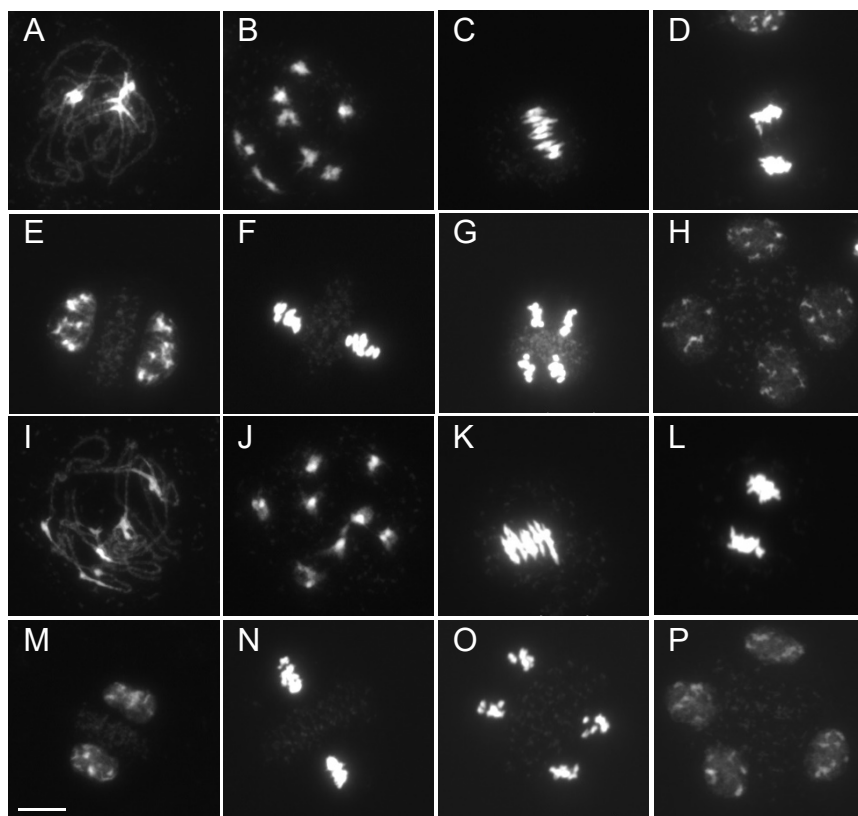
(A) Venn diagrams showing overlap of deregulated genes ($|\log_2 \text{fold change}| > 1$, $p < 0.05$) in *nRPD1* microspores of *Capsella* and genes losing 21/22-nt and 24-nt siRNAs at 2kb up-and downstream and gene body ($\log_2 \text{fold change} < -1$, $p < 0.05$) in *Capsella nRPD1* microspores.

(B) Enriched gene ontologies (GO) for biological processes of intersected genes losing siRNAs and deregulated genes in *Capsella nRPD1* microspores. Top 5 GOs of each analysis are shown.

(C) Distance of *Arabidopsis* and *Capsella* genes to closest TEs. All: all genes, up: significantly upregulated genes, down: significantly downregulated genes. * $p < 0.05$, ** $p < 0.01$, *** $p < 0.001$, n.s, not significant. (Statistical analysis: Wilcoxon test).

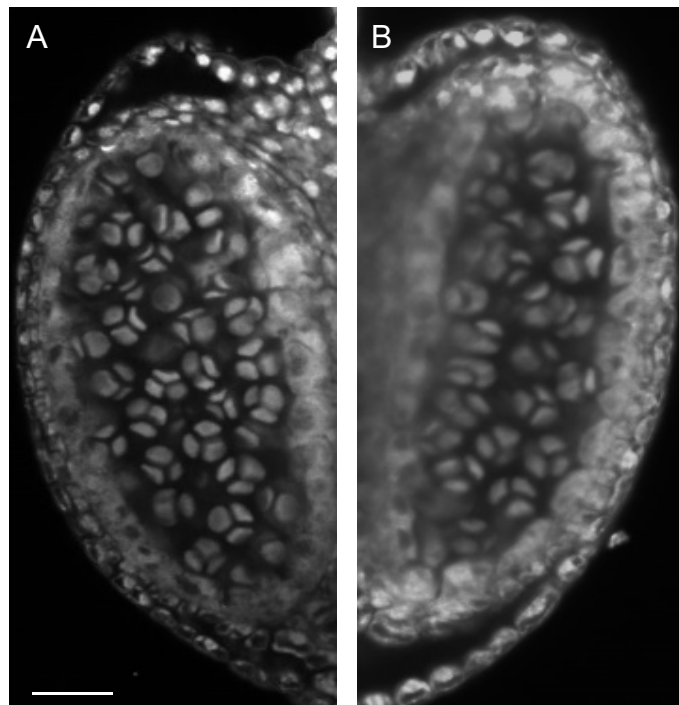
(D) Log₂ expression fold change of, PRK2, PRK3, PRK4, RopGEF9, VGD1 and ANX2 genes in *nRPD1* microspores compared to wild type (wt) in *Capsella* (Cr) and *Arabidopsis* (At).

(E) mRNA levels of PRK2, PRK3, PRK4, RopGEF9, VGD1 and ANX2 in *Arabidopsis* wild-type meiocytes, microspores and mature pollen grain (MPG). We added plus1 to all values to avoid negative log₁₀ values.



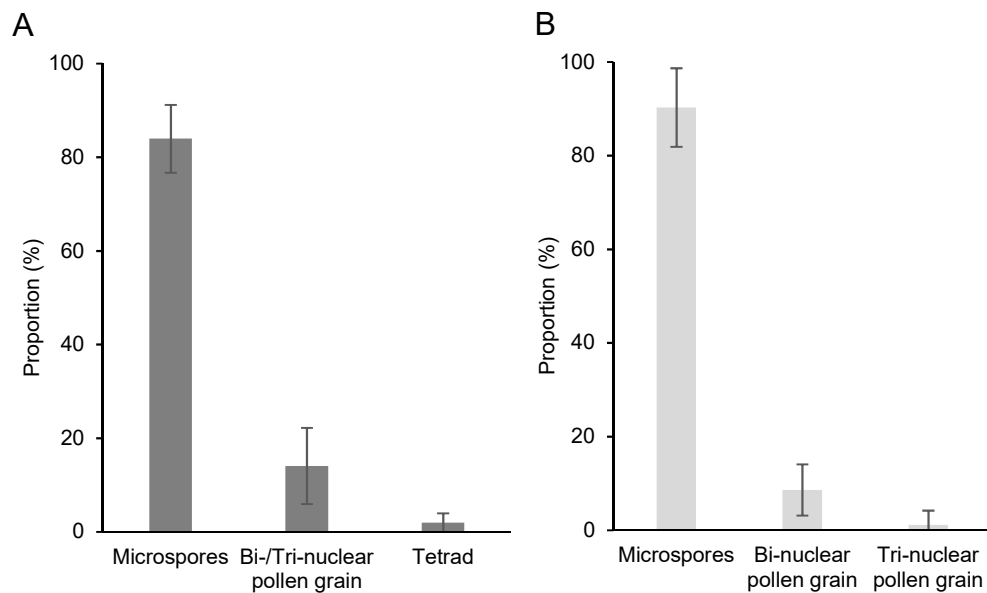
Supplemental Figure 1. Meiosis is not affected in *Capsella nrpd1*. Supports Figure 2.

Meiosis in *Capsella* wild-type (A - H) and *nrpd1* (I - P) plants. A and I, pachytene. B and J, diakinesis. C and K, metaphase I. D and L, telophase I. E and M, prophase II. F and N, metaphase II. G and O, anaphase II. H and P, telophase II. Bar: 5 μ m.



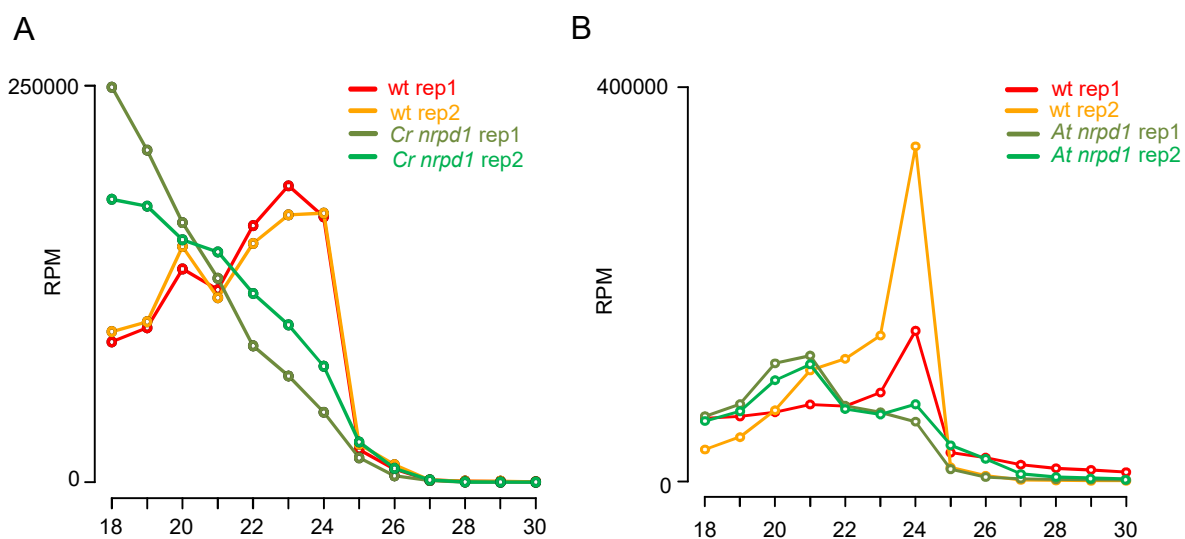
Supplemental Figure 2. Normal tetrad formation in *Capsella* wild type (A) and *nrpd1* (B). Supports Figure 2.

Shown are whole mount confocal images. Bar: 20 μ m.

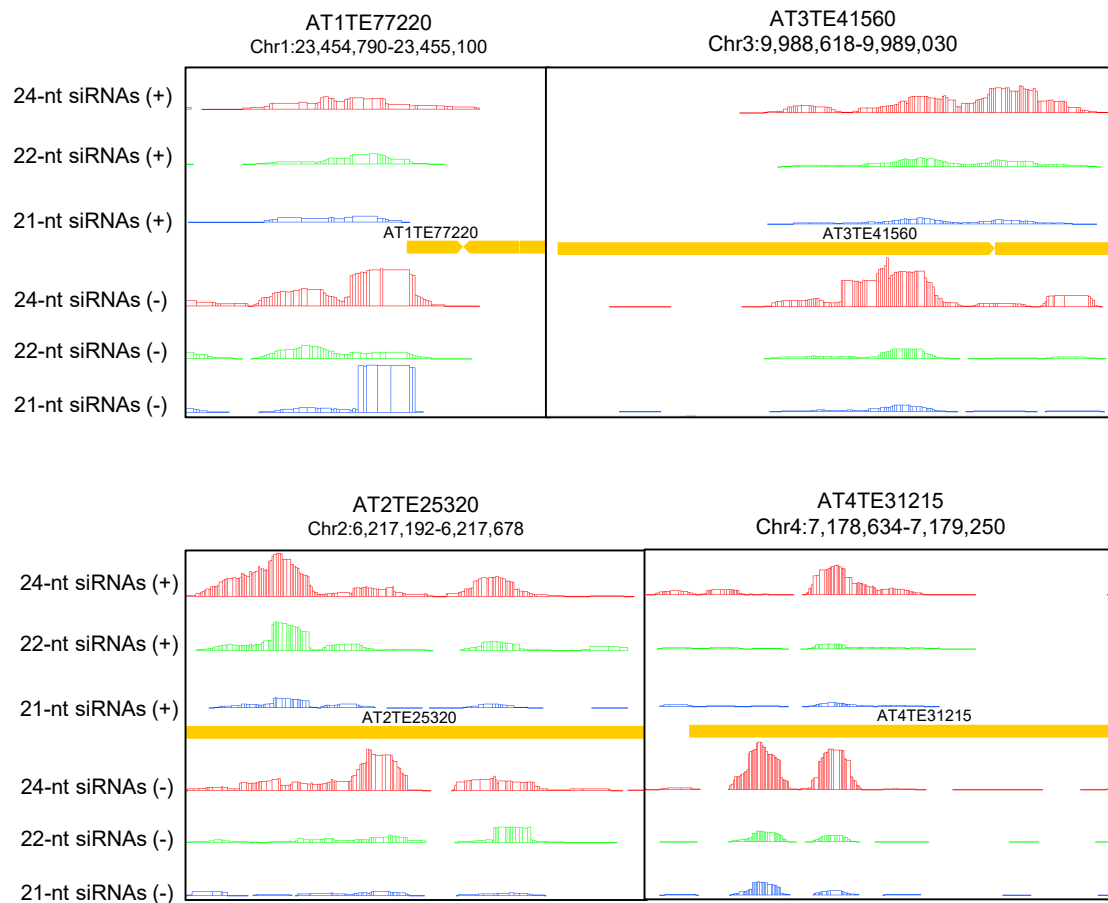


Supplemental Figure 3. Average purity of *Capsella* and *Arabidopsis* microspore extractions. Supports Figure 4.

Microspore extractions of *Capsella* (A) and *Arabidopsis* (B) were tested by DAPI staining and the B2 and B1 fractions were selected as the fractions containing the highest proportion of microspores in *Capsella* and *Arabidopsis*, respectively. Shown is the average percentage of four and eight independent extractions in *Capsella* and *Arabidopsis*, respectively. Error bars show standard deviation.

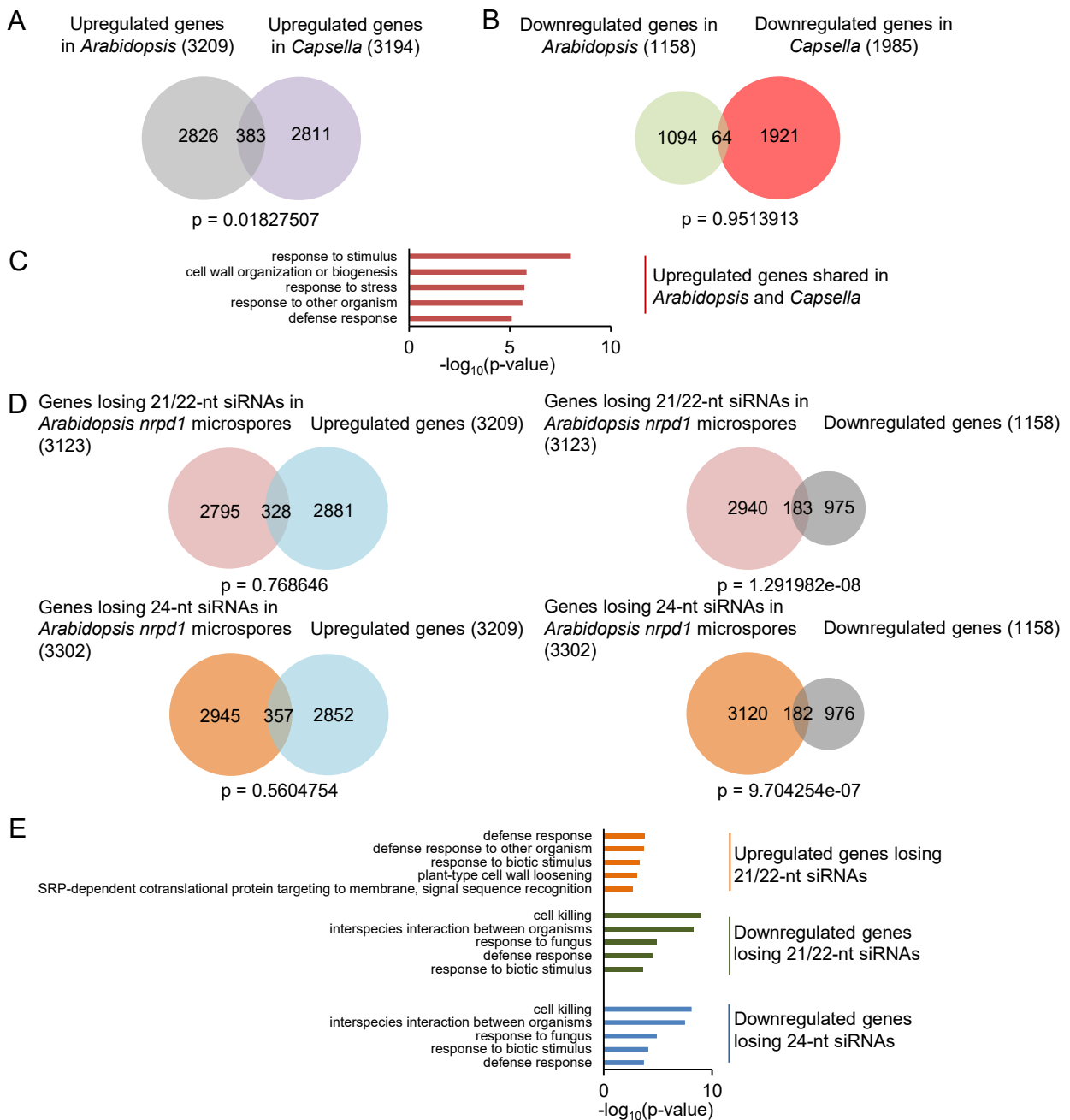


Supplemental Figure 4. Profile of total sRNAs in *Capsella* (A) and *Arabidopsis* (B) microspores. Supports Figure 4.



Supplemental Figure 5. Examples of four loci producing Pol IV-dependent siRNAs in *Arabidopsis*. Supports Figure 6.

Bars represent normalized reads. The color indicates the length of the analyzed reads: red 24-nt, blue 22-nt, and green 21-nt. The DNA strand is indicated by the (+) or (-). TE sequences are represented in yellow.



Supplemental Figure 6. Deregulated genes in *Arabidopsis nrpd1* mutant microspores. Supports Figure 8.

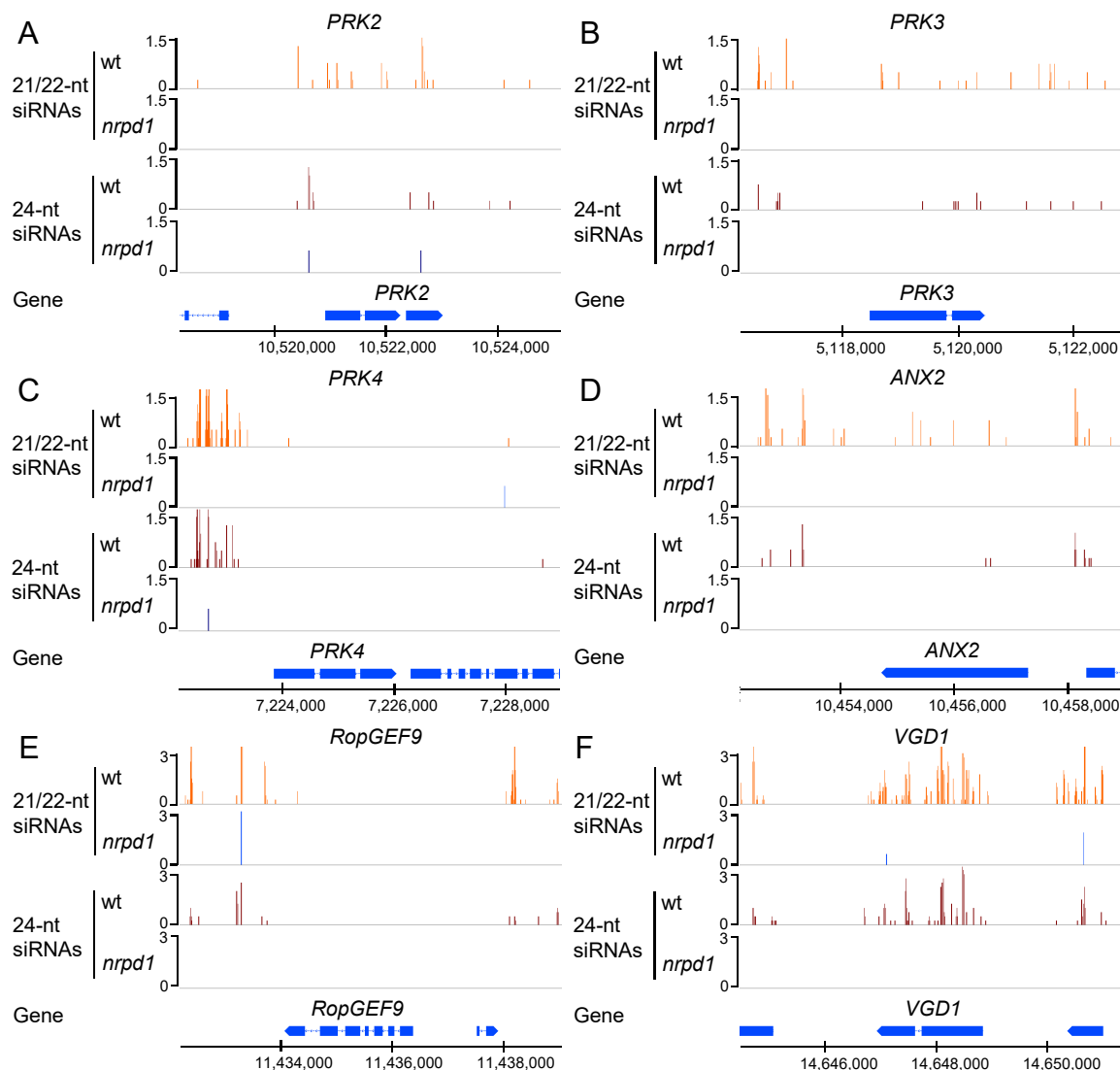
(A) Venn diagram showing overlap of upregulated genes in *nrpd1* microspores of *Capsella* and *Arabidopsis*. Significance was determined by a hypergeometric test.

(B) Venn diagram showing overlap of downregulated genes in *nrpd1* microspores of *Capsella* and *Arabidopsis*. Significance was determined by a hypergeometric test.

(C) Enriched gene ontologies (GO) for biological processes of upregulated genes shared in *Arabidopsis* and *Capsella nrpd1* microspores. Top 5 GOs with $p < 0.01$ are shown.

(D) Venn diagrams showing overlap of deregulated genes ($|\log_2 \text{fold change}| > 1$, $p < 0.05$) in *nrpd1* microspores of *Arabidopsis* and genes losing 21/22-nt and 24-nt siRNAs at 2kb up-and downstream and gene body ($\log_2 \text{fold change} < -1$, $p < 0.05$) in *Arabidopsis nrpd1* microspores. Significance was determined by a hypergeometric test.

(E) Enriched gene ontologies (GO) for biological processes of intersected genes losing siRNAs and deregulated genes in *Arabidopsis nrpd1* microspores. Top 5 GOs with $p < 0.01$ are shown.



Supplemental Figure 7. Representative pollen developmental genes accumulating 21/22-nt and 24-nt siRNAs in *Capsella* microspores.

Supplemental table 1. Primer list

Primer names	Sequences	Application
CrT1 NRPD1	ATATATGGTCTCGATTGAATCCTTCTGCGATCGTCGTTT AGAGCTAGAAATAGC	Generate Crispr/cas9 construct for pol iv
CrT2 NRPD1	ATTATTGGTCTCGAAACGATAAGCTCCGTCAAGCTACAA TCTCTTAGTCGACTCTAC	Generate Crispr/cas9 construct for pol iv
pHEE401E-Seq-F	GTTGTAAAACGACGCCAGT	Sequencing Crispr/cas9 construct
pHEE401E-Seq-R	CAAACGCAAATGCTTTATTCAC	Sequencing Crispr/cas9 construct
Cr-NRPD1-seq-F	GTTCTCGTGTGGTCGAATGC	PCR for identifying pol iv mutation
Cr-NRPD1-seq-R	CTCATAGCAGAACCGAGCCA	PCR for identifying pol iv mutation
At_NRPD1_F	GGGGACAAGTTGTACAAAAAAGCAGGCTATGGAAGACGATTGT GAGGAGC	For cloning Arabidopsis NRPD1
At_NRPD1_F	GGGGACCACTTGTACAAGAAAGCTGGGTCACGGGTTTCGGA GAAACC	For cloning Arabidopsis NRPD1

Supplemental table 2. Quality of sequencing samples.

Table shows details of the sequenced samples generated in this study. Replicates are biological replicates.

sRNAs-seq		Raw reads	Reads after trimming	% Reads after trimming	Structural RNAs (removed)	Nr. of mapped reads	% Mapped reads
Arabidopsis microspores							
Col-0	Replicate 1	11209095	6753162	60.2	2489434	1444728	33.9
Col-0	Replicate 2	10665337	8098812	75.9	2921468	2771963	53.5
<i>nRPd1</i>	Replicate 1	9494296	6450194	67.9	3453871	815700	27.2
<i>nRPd1</i>	Replicate 2	12788162	9326033	72.9	4726264	1100282	23.9
Capsella microspores							
wt	Replicate 1	37486299	17981812	48.0	3925936	4612276	32.8
wt	Replicate 2	45960996	24914782	54.2	5574458	6802012	35.2
<i>nRPd1</i>	Replicate 1	38517066	10699950	27.8	4953248	1839721	32.0
<i>nRPd1</i>	Replicate 2	28406775	12768877	45.0	5995670	2415118	35.7
Capsella leaves							
wt	Replicate 1	27409329	16846352	61.5	5122709	3597197	30.7
wt	Replicate 2	22259993	14208445	63.8	4161497	3302984	32.9
<i>nRPd1</i>	Replicate 1	16003678	8919400	55.7	2748976	1830154	29.7
<i>nRPd1</i>	Replicate 2	38120832	23880822	62.6	7534940	4934084	30.2
mRNA-seq		N of total reads	N of reads mapped	% map efficiency			
Arabidopsis microspores							
Col-0	Replicate 1	43062744	32065947	74.5			
Col-0	Replicate 2	38810670	25694591	66.2			
<i>nRPd1</i>	Replicate 1	44286782	30779621	69.5			
<i>nRPd1</i>	Replicate 2	53713266	40653906	75.7			
Capsella microspores							
wt	Replicate 1	60915596	25989393	42.7			
wt	Replicate 2	58387014	29983324	51.4			
<i>nRPd1</i>	Replicate 1	72911086	34311091	47.1			
<i>nRPd1</i>	Replicate 2	68671724	30759236	44.8			
Bisulfite-seq							
Capsella leaves							
		N of trimmed reads R1	N of mapped reads R1	map efficiency %	Genome Coverage	non-conversion	rates %
wt	Replicate 1	31169177	11598232	37.2	5.4	0.5	
wt	Replicate 2	34936119	13801777	39.5	6.2	1.4	
<i>nRPd1</i>	Replicate 1	29591259	11329390	38.3	5.2	0.6	
<i>nRPd1</i>	Replicate 2	35716742	13160912	36.8	6.0	0.5	
WGS							
Capsella leaves							
		N of total read pairs	coverage				
wt		42815402	68x				
<i>nRPd1_1</i>		39261629	41x				
<i>nRPd1_2</i>		33173870	44x				
<i>nRPd1_3</i>		32911305	52x				
<i>nRPd1_4</i>		45561371	65x				
<i>nRPd1_5</i>		31298911	48x				